Scientific Contributions Oil & Gas, Vol. 48. No. 4, December: 273 - 301

SCIENTIFIC CONTRIBUTIONS OIL AND GAS

Testing Center for Oil and Gas
LEMIGAS

Journal Homepage:http://www.journal.lemigas.esdm.go.id
ISSN: 2089-3361, e-ISSN: 2541-0520

Comparative Study of Capacitance Resistance Model and Machine Learning for Sensitivity Analysis of Polymer Injection Performance

Azri Agus Rizal, Fajril Ambia, Novia Rita, and Ira Herawati

Department of Petroleum Engineering, Faculty of Engineering, Universitas Islam Riau
Kaharuddin Nasution Street 113, Simpang Tiga, Pekanbaru, Riau, 28284, Indonesia.

Corresponding Author: Fajril Ambia (fajril@eng.uir.ac.id)

Manuscript received: October 20th, 2025; Revised: November 06th, 2025
Approved: December 05th, 2025; Available online: December 17th, 2025; Published: December 18th, 2025.

ABSTRACT - The objective of this study was to evaluate the performance of polymer injection in the Volve Field by validating full-physics Navigator simulation results. This process was performed using two independent data-driven approaches: the Capacitance resistance model (CRM) and machine-learning algorithms Random Forest and XGBoost. This validation framework addresses uncertainty in flow-parameter and ensures that simulated production responses align with data-driven injection–production behavior. The simulation model was constructed using 20 years of historical field data, consisted of five years of polymer injection at 1000–3000 ppm, followed by 15 years of chase water flooding. The simulation results showed that polymer injection increased the oil recovery factor from 21.12% to 21.30% in the best-case scenario, indicating a modest improvement in sweep efficiency. CRM, applied through CRM-P and CRM-IP configurations, successfully reconstructed production profiles and quantified interwell connectivity (R^2 = 0.94; MAPE < 10%). Machine-learning validation further confirmed these results, with Random Forest achieving R^2 = 0.92 (MAPE < 1%) and XGBoost achieving R^2 = 0.99 (MAPE < 1%). Overall, CRM and machine learning provide effective and independent validation pathways, enhancing confidence in simulation outcomes and allowing for reliable assessment of polymer-injection performance in field applications.

Keywords: polymer injection, CRM, DCA, machine learning, xgboost, random forest, EOR, volve field.

How to cite this article:

Azri Agus Rizal, Fajril Ambia, Novia Rita, and Ira Herawati 2025, Comparative Study of Capacitance Resistance Model and Machine Learning for Sensitivity Analysis of Polymer Injection Performance, Scientific Contributions Oil and Gas, 48 (4) pp. 273 - 301. DOI org/10.29017/scog.v48i4.1929 .

INTRODUCTION

Polymer flooding is one of the most widely applied chemical enhanced oil recovery (EOR) methods due to its ability to improve mobility ratio, reduce water cut, and increase macroscopic sweep efficiency in mature fields (Alvarado & Manrique 2010). Despite its potential, predicting polymer-injection performance remains highly challenging. Reservoir heterogeneity, polymer thermal degradation, salinity effects, and uncertainties in interwell flow behavior often cause polymer floods to perform below expectations (Khalbia, 2021; M. H. Nugroho et al., 2021).

These challenges complicate the interpretation of observed production trends and limit the ability of operators to determine whether polymer injection is genuinely effective or simply behaving like a conventional waterflood. In practice, full-physics reservoir simulation is commonly used to model polymer flooding performance; however, the simulation results must be validated. Numerical models may suffer from parameter uncertainty, non-unique history matching, and simplifications in representing polymer rheology, adsorption, and retention. For these reasons, data-driven diagnostic tools are increasingly required to independently verify whether production responses predicted by simulation align with actual interwell dynamics. Without such validation, decision-making for polymer optimization are uncertain and prone to error.

The capacitance resistance model (CRM) has emerged as an efficient analytical method for characterizing injector–producer connectivity and reservoir response time using only historical rate fluctuations (Sayarpour et al., 2008; Weber 2009). CRM enables rapid screening of interwell communication patterns and provides insights into whether the injected polymer is influencing production wells as intended.

However, CRM is also sensitive to assumptions and data sparsity, making independent validation necessary, particularly in reservoirs with strong heterogeneity. Machine learning provides a complementary, independent validation approach. Random Forest and XGBoost are Algorithms that can learn nonlinear relationships between injection and production variables without relying on predefined physical assumptions (Imankulov et al., 2022; Shang et al., 2023). In this research, machine learning is neither integrated or coupled with CRM. Instead, these methods are used independently to benchmark and validate the production responses generated by the tNavigator polymer simulation model. By comparing CRM outputs, machine-learning predictions, and simulation results, a more reliable interpretation of polymer performance can be achieved.

Therefore, the purpose of this study is to evaluate polymer injection performance in the Volve Field by using two independent data-driven diagnostic methods, the Capacitance Resistance Model and machine learning, to validate reservoir simulation results. This approach addresses the gap commonly found between simulated and actual reservoir behavior, reduces interpretational uncertainty, and provides a more robust framework for assessing the true effectiveness of polymer flooding in heterogeneous reservoirs.

METHODOLOGY

This research began with reservoir simulation using Tnavigator to display historical production data and injection flow rates from polymer injection in a real field model. This data was used to understand the impact of polymer injection on fluid flow in the reservoir. This was followed by the development of the capacitance resistance model (CRMP) and (CRMIP) algorithms using the Python programming language. This process included history matching to compare CRM model predictions with actual field data, where accuracy was assessed using R^2 and Mean absolute percentage error (MAPE) metrics. To improve the analysis, this study utilized machine learning methods, specifically Random Forest and XGBoost, to execute historical matching predictions using data from the Volve Field. By comparing the results from CRM models and machine learning techniques, which one provides more accurate predictions is identified.

Capacitance resistance model

The capacitance resistance model (CRM) is a technique commonly used to model the dynamic relationship between the injection and production rates of wells. This model applies an electrical resistor-capacitor circuit analogy to represent the delay and connectivity behavior between production and injection wells based on historical data. The main advantage of CRM is its ability to predict reservoir performance with simpler calculations compared to complex numerical simulation approaches (Sayarpour et al., 2009).

CRMP : producer-based representation

The CRMP is a model built with producers as the center or focus of the model control system. In this scheme, each production well is analyzed individually to achieve higher resolution (de Holanda et al., 2018). The CRMP (producer-based representation) considers one time constant (τ_j) and one productivity index (J_j) for each producer and one interwell connectivity for each pair of injector wells (i) – producer wells (j). Accordingly, the governing equation can be represented as follows:

$$\tau_j \frac{dq_j}{dt} + q_j(t) = \sum_{i=1}^{Ninj} f_{ij}\, i_i(t) - \tau_j J_j \frac{dp_{wf}^{(j)}}{dt} \qquad (1)$$

CRMIP : injector-producer based representation

CRMIP is the most recent CRM model to consider reservoir heterogeneity. Heterogeneity in this model referes to different individual/pair parameters, hence assuming a single value for all producers or reservoirs is not reliable. Therefore, the continuity equation of in CRMIP will be written based on a representation based on injector well-producer well pairs and their control systems.

Each pair has a single time constant (τ_{ij}), productivity index (J_{ij}), and interwell connectivity (f_{ij}) for each injector (i) -producer (j) pair. The ODE for this pair-based control volume can be written as follows (de Holanda et al., 2018).

$$\tau_{ij} \frac{dq_j}{dt} + q_{ij}(t) = f_{ij}\, i_i(t) - \tau_{ij}\, J_{ij} \frac{dp_{wf}^{(j)}}{dt} \qquad (2)$$

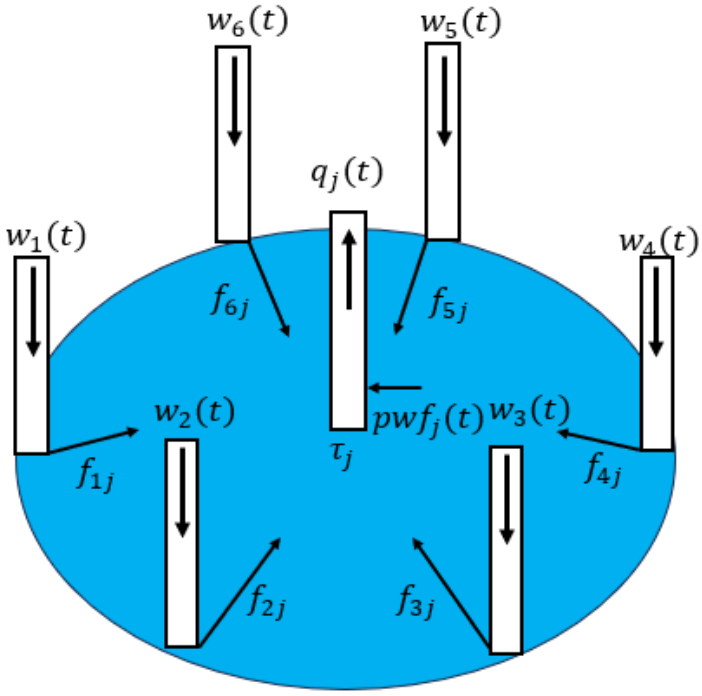

Figure 1. CRMP – *Producer-based Representation*

Where qij represents the production rate (bpd) at the producer relative to the control volume of the injector (i)-producer (j) pair. Thus, the total production flow rate of producer j is obtained by summing all production flow rates contributed by its respective control volumes.

In this study, the Capacitance resistance model (CRM) was employed to validate the tNavigator simulation results through two main configurations, CRM-P and CRM-IP. CRM-P models the production rate of each producer well by linking production fluctuations to the combined effects of injection support and the internal decline dynamics of the well, allowing the reservoir response characteristics to be quantified through the time constant (ô). Meanwhile, CRM-IP computes the interwell connectivity (f_{ij}) for each injector–producer pair to identify the flow pathways and the influence of individual injectors on production. When combined, these configurations enable an assessment of whether the connectivity patterns and production responses predicted by the tNavigator simulation are consistent with the data-driven reservoir behavior reconstructed by CRM, providing a more comprehensive validation of polymer-injection performance.

Decline curve analysis

Decline curve analysis (DCA) is a simple and easy-to-use method that is widely used to predict future production rates and oil reserves. This method requires the availability of production data, which is then used to identify decline trends using empirical equations. Using these trends, we may predict future production (Maurenza et al., 2023).

$$q = q_i e^{(-D_i \Delta t)} \quad (3)$$

Machine learning

Machine learning methods, such as Random Forest and XGBoost, have been proven to be effective in analyzing large and complex data sets found in reservoirs. As demonstrated by (Zhao & Liu 2023), this algorithm is capable of capturing complex and nonlinear patterns in data, which is often difficult to achieve using traditional methods.

Random Forest uses an ensemble of many decision trees (Hidayat & Astsauri 2021), resulting in more accurate decision-making and reduces overfitting, while XGBoost provides an advanced optimization approach that can further improve prediction accuracy (Yan et al., 2023). These two machine learning algorithms use past production and injection data, as well as other reservoir parameter variables, to provide robust predictions and anticipate potential production uncertainty.

Integrated polymer simulation tnavigator

The objective of this research is to evaluate the performance of polymer injection in the Volve Field by validating reservoir simulation results through two independent data-driven approaches: the capacitance resistance model (CRM) and machine-learning prediction. Both CRM and machine-learning models are applied separately to assess whether the production responses generated by the tNavigator

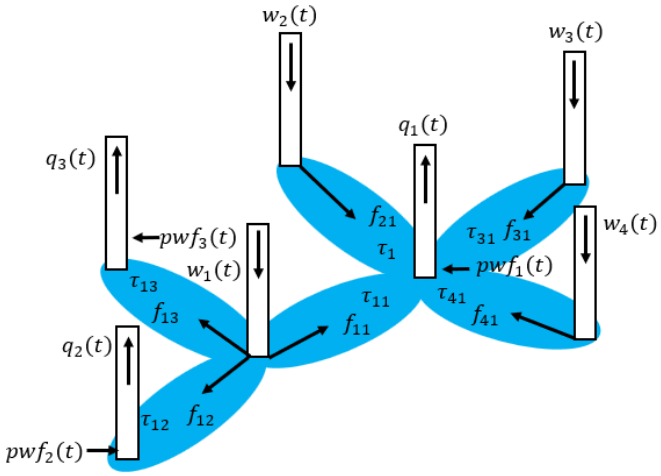

Figure 2. CRMIP: *Injector-Producer Based Representation*

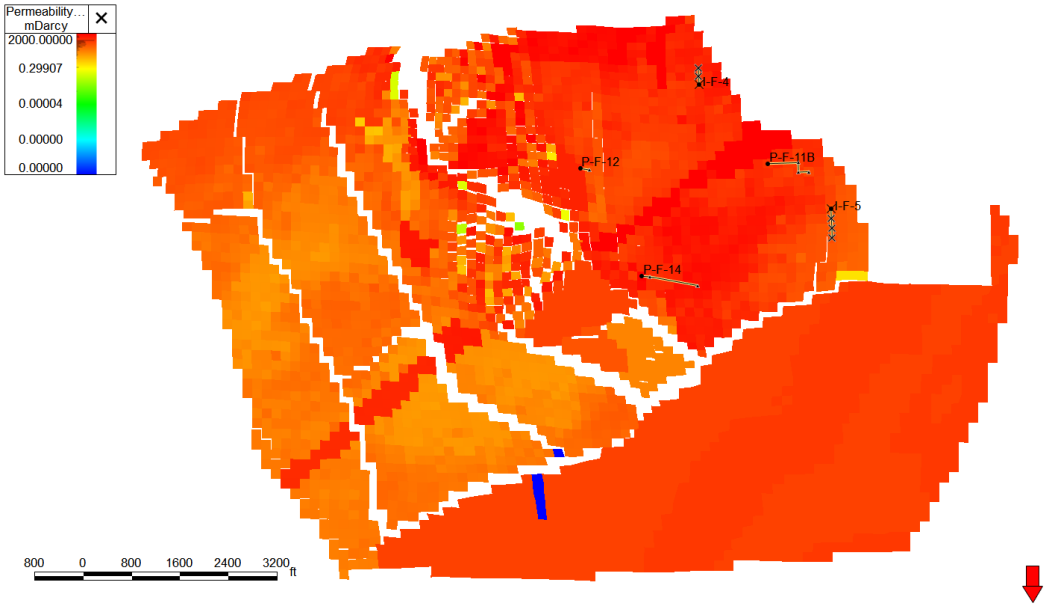

Figure 3. 2D Visualization of the permeability distribution in the volve field

simulation are consistent with the data-driven behavior inferred from historical injection–production dynamics. The workflow begins with constructing a 3D reservoir simulation model in tNavigator, followed by history matching of the waterflood phase with an error below 0.5%. The polymer injection stage is then simulated using the POLYMER keyword with concentrations of 1000–3000 ppm for 5 years, followed by 15 years of chase water, totaling 20 years of simulation.

Two injection wells were operated at a constant rate of 1,500 bbl/day. The optimal scenario was selected based on the highest recovery factor, after which the simulation results were exported for CRM and machine-learning analysis. For the CRM workflow, the tNavigator production data were used to estimate interwell connectivity (f_{ij}) and time constants (ô), which were subsequently used to generate CRM-based production forecasts.

In parallel, machine-learning models Random Forest and XGBoost were trained using the same injection–production dataset utilizing a well-based split evaluation. These models were not used to validate CRM history matching; instead, they served as independent predictive benchmarks to compare directly against both CRM forecasts and the original simulation results. By applying CRM and Machine learning as two independent validation pathways, this methodology provides a robust assessment of whether the tNavigator polymer-flood simulation realistically captures the underlying injection - production behavior of the Volve Field.

RESULT AND DISCUSSION

In this study, the initialization and simulation of the Volve field model were carried out using tNavigator, with history matching or matching of actual production history was performed between early 2015 and 2024. The Volve field has undergone water injection since 2015. After that, the simulation model was forecasted for 20 years as a base case for waterflood injection starting from 2024 to 2044 and then continued with a polymer slug injection scenario for 5 years and followed by chase water injection for 15 years.

To accurately characterize fluid flow behavior in reservoirs, it is essential to model the permeability distribution. As illustrated in Figure 3, the permeability map of the Volve field highlights the reservoir's heterogeneity, characterized by variations in permeability values.

Most of the reservoir has good permeability. A clear contrast can be observed between the highly productive main flow zones, where permeability reaches up to 2000 mD (represented by red and orange colors), and the low-permeability or barrier zones, where permeability

Table 1. Initialization of the 3D volve field model

Parameter	Nilai	Satuan
Original Oil in Place	76.9942	MMSTB
Original Water in Place	697.7655	MMSTB
Original Gas in Place	55.2871	MMSCF
Pore Volume	794.7169	Million RB

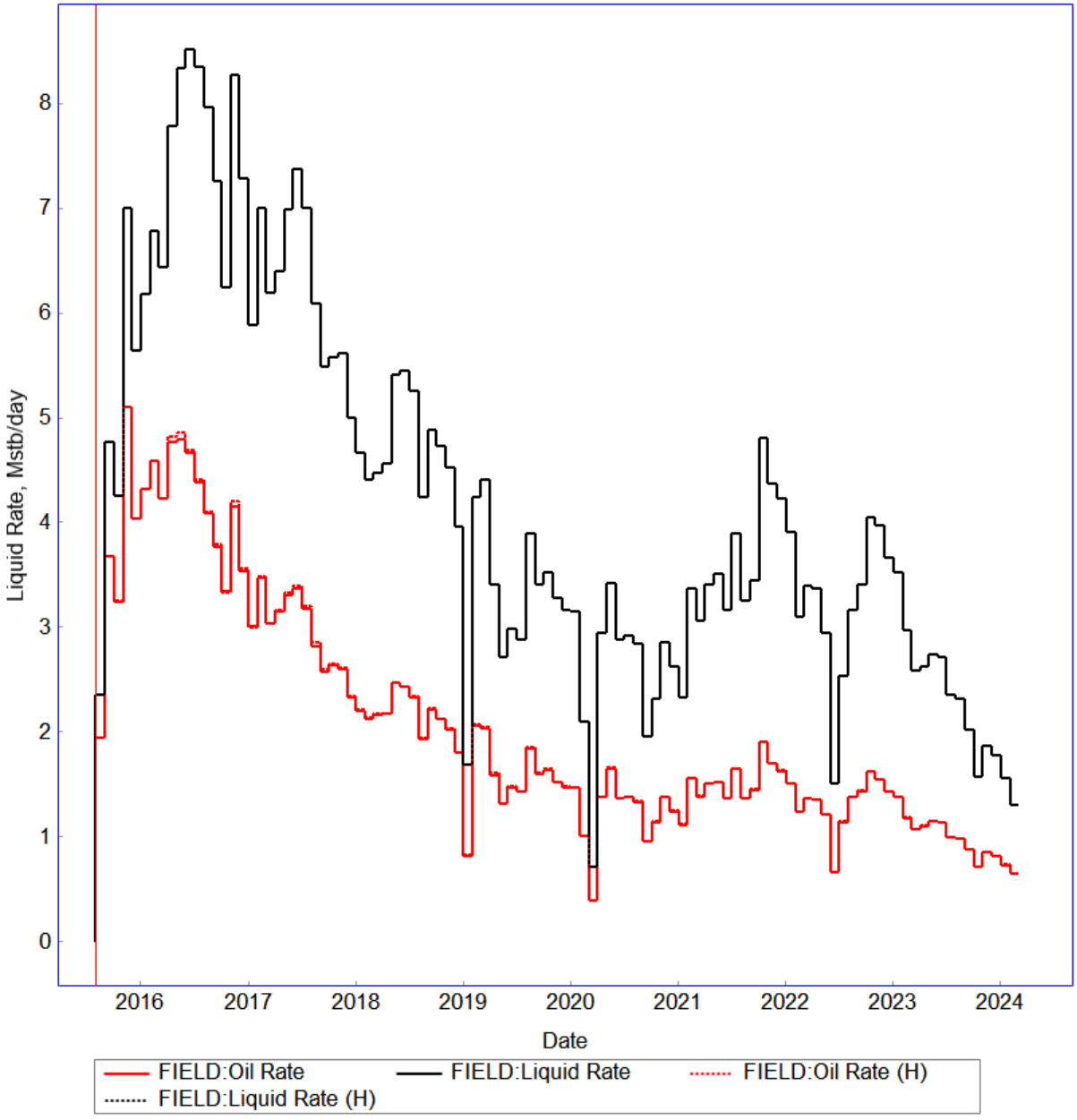

Figure 4. History matching the volve field production

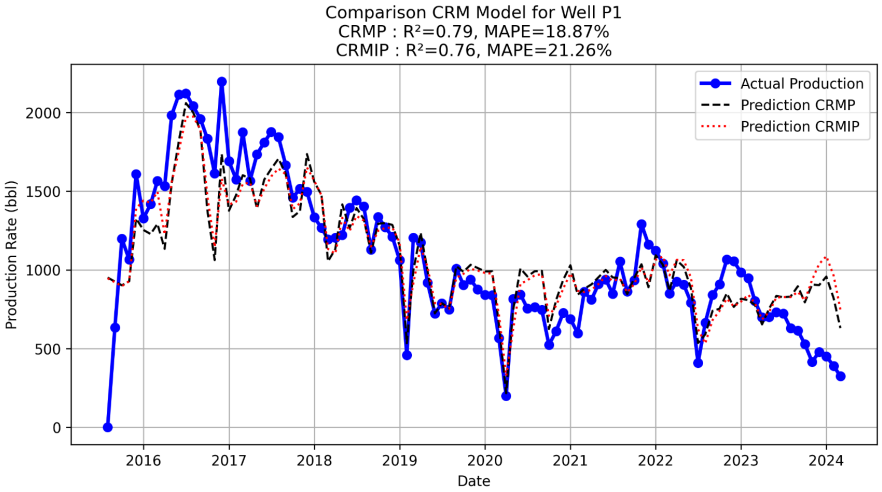

Figure 5 (a)

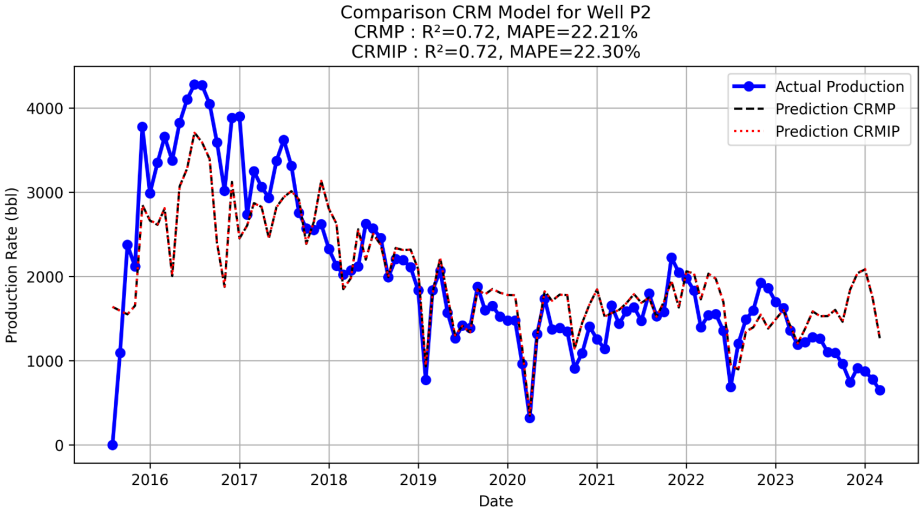

Figure 5 (b)

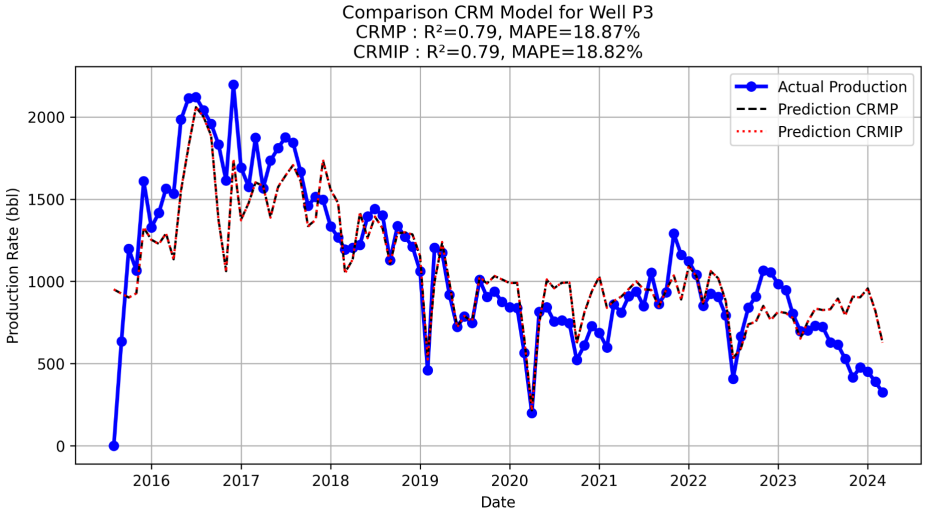

Figure 5 (c)

Figure 5. History matching and validation of waterflood injection using CRM method in the volve field (a)Well P1 (b) Well P2 (c) Well P3

approaches zero (depicted in blue). Reservoir model initialization began with a history match of actual field production data. The results are shown in Figure 4. This history matching shows excellent agreement between the simulation data (solid line) and historical field data (markers). The model accurately replicated the production decline trend for both oil and liquid rates. This indicates that the model has been well validated and is capable of accurately representing reservoir behavior.

Analysis, history matching, and validation CRM for water injection

The history matching process conducted to estimate CRM parameters (interwell connectivity and time constant) showed very satisfactory results in curve fitting for the independent variable of injection water flow rate (Salehian & Çýnar 2019). The CRMP model (black line) and the CRMIP model (red line) show excellent agreement with actual data from tNavigator simulations, as confirmed by research which shows that CRM can predict future oil recovery with less than 2% difference compared to simulation results (Davudov et al., 2020). Overall, the history-matching results from the three wells (P1, P2, and P3) indicate that the capacitance-resistive model (CRM) is highly effective in replicating historical production data (M. H. Nugroho et al., 2021).

With R^2 values ranging from 0.72 to 0.79, this model demonstrates a strong ability to explain most of the variability in production. The model successfully separates two main phenomena: the natural decline in reservoir production and the significant, fluctuating increase in output in response to injection activity (modeled by CRM) (Lesan et al., 2018. Wells P1 and P3 show a very high degree of accuracy, indicating that the behavior of the surrounding reservoir can be predicted well by the model, while the slightly lower but still acceptable fit for well P2 indicates

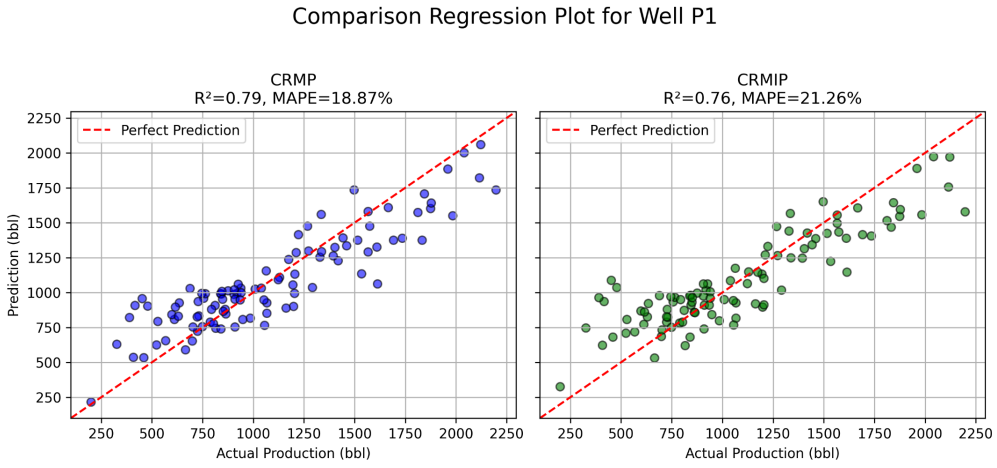

Figure 6 (a)

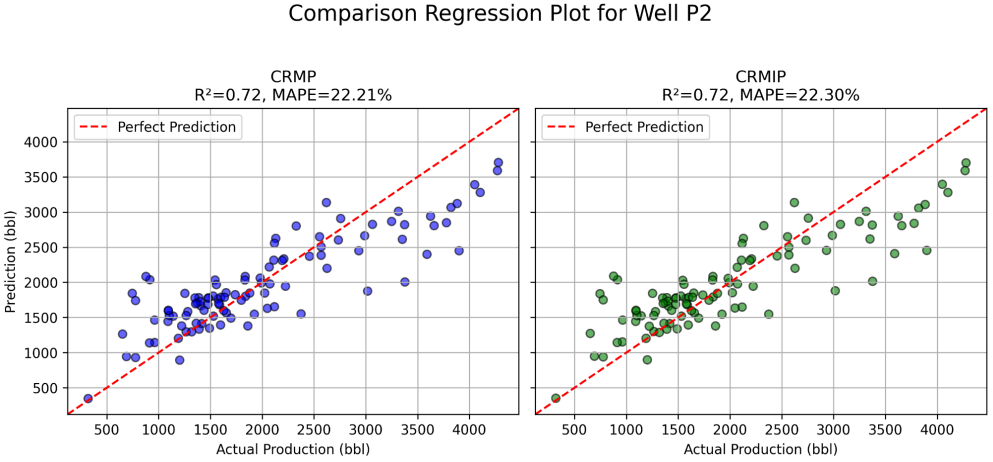

Figure 6 (b)

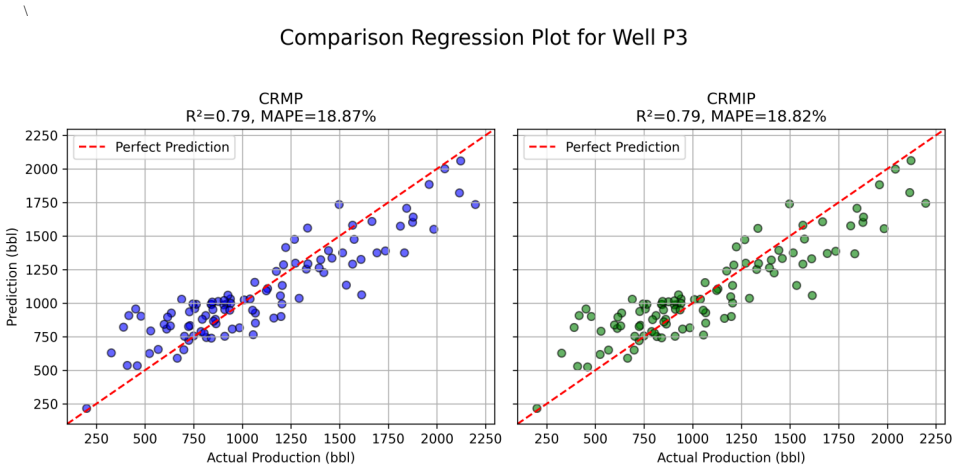

Figure 6 (c)

Figure 6. Comparison of the regression plot CRMP, and CRMIP for well production (a) well P1 (b) well P2 (c) well P3

higher geological complexity or fluid dynamics (Nwogu et al., 2019). As shown in Figure 6, the regression plots collectively provide strong visual validation of the performance of the CRMP and CRMIP models. It is clear that both models successfully demonstrate a strong linear correlation, marked by data distribution concentrated along the "Perfect Prediction" line. This confirms that there is no significant systematic bias (consistent over-prediction or under-prediction) in the model results. It is also confirmed that R^2 provides a high score only when the majority of elements have been predicted correctly (Chicco et al., 2021). The high of R^2 value, ranging from 0.72 to 0.79, indicates that the model is able to explain more than 72% of the variation in production data. In addition, the relatively small MAPE value (less than 23%) proves that the margin of error in the model's predictions is still acceptable.

Table 2. Interwell connectivity dan time constant CRMP

Well production	Well injection		Time constant τ (days)
	I1	I2	
P1	0.006679	0.009858	30
P2	0.019587	0.011147	30
P3	0.006679	0.009858	30

Table 3. Interwell connectivity CRMIP

Well production	Well injection	
	I1	I2
P1	0.0094	0.0064
P2	0.0191	0.0109
P3	0.0067	0.0099

Table 4. Time constant CRMIP

Well production	Well injection	
	I1	I2
P1	32	30.55
P2	30.86	30.54
P3	30	30

Tables 2, 3, and 4 summarize the capacitance resistance model (CRM) parameters during the water injection phase at the Volve Field. This comparison provides an overview of the relationship between wells (interwell connectivity) and the reservoir response time (time constant).

The results of the capacitance resistance model (CRM) indicate a consistent pattern of connectivity between wells, along with notable variations in time constants. Connectivity analysis shows that production well P2 has the strongest connection with injector I1, while wells P1 and P3 show more dominant connectivity with injector I2 (Fu et al., 2022). The main difference lies in the approach to the time constant ô. The CRMP model uses a simplified approach with a single value of 30 days for the entire system, while the CRMIP model provides a more detailed representation by calculating variable time constants for each well pair, ranging from 30 to 32 days (Abbasov et al., 2023). The CRMIP approach is physically more realistic since it considers reservoir heterogeneity, which is an important characteristic in complex waterflooding systems. The CRM method has proven effective in understanding the dynamic interaction between injection and production wells

without requiring complex numerical modeling, so it can be used for optimization of operating parameters and production forecasting (Fu et al., 2022; Pyatibratov & Zammam 2023).

Figure 7 presents a 3D visualization of the interwell connectivity parameters derived from the CRM Model. This map illustrates the spatial distribution of injection and production wells, as well as the strength of the hydraulic relationship between them. The thickness of the arrows represents the magnitude of the connectivity values.

From this image, the main flow patterns can be clearly identified. The strongest connection is observed between Injector I1 and Producer P2, marked by the thickest arrow. In contrast, Injector I2 exerts a more dominant influence on Producers P1 and P3, while the impact of Injector I1 on these producers is minimal. This visualization effectively summarizes the quantitative results of the model and provides an intuitive understanding of the reservoir depletion pattern.

Analysis of machine learning, random forest, and gradient boosting for water injection

Figure 8 shows the results of the Random forest prediction evaluation on the training data, demonstrating a very high level of accuracy. The model achieved a coefficient of determination R^2 of 0.98 and a very low MAPE of 6.17% for well P1 and 5.81% for well P2. These metrics quantitatively prove that the model is capable of replicating more than 98% of historical data variability with a minimal average error. On a previously unseen validation dataset (P3), the model maintained a very high level of accuracy with R^2 = 0.98 and MAPE = 6.17%. These validation results show that the model successfully learned the underlying production patterns without overfitting. On the regression plot, the distribution

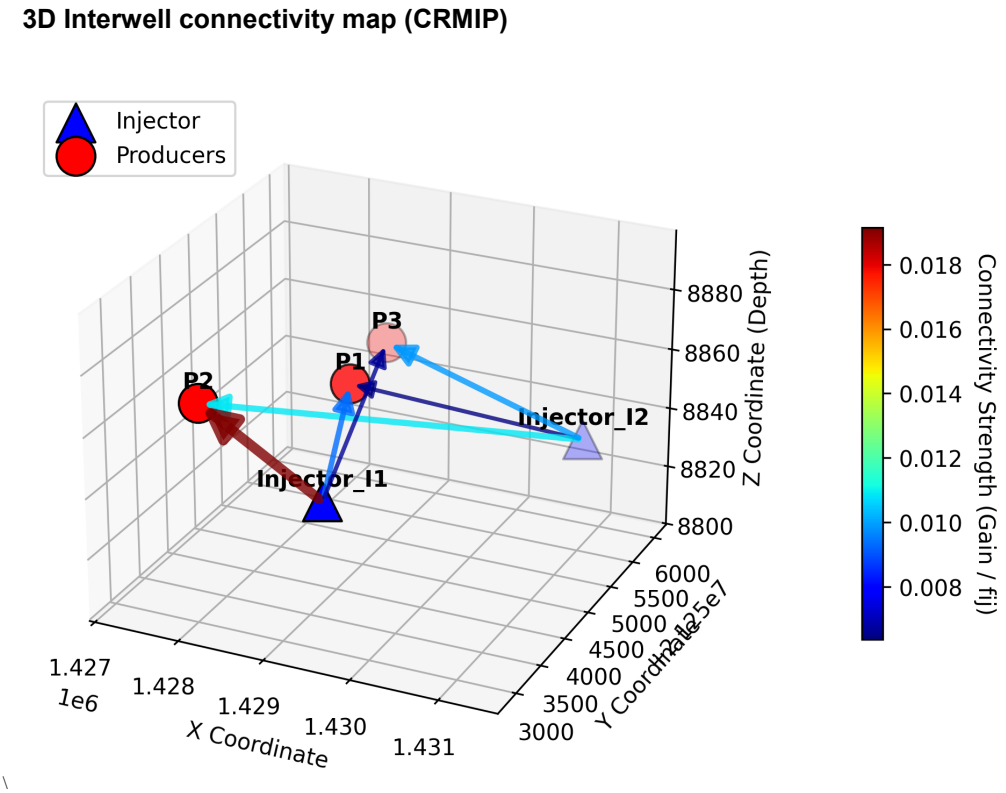

Figure 7. 3D Interwell Connectivity Map in Volve Field Model

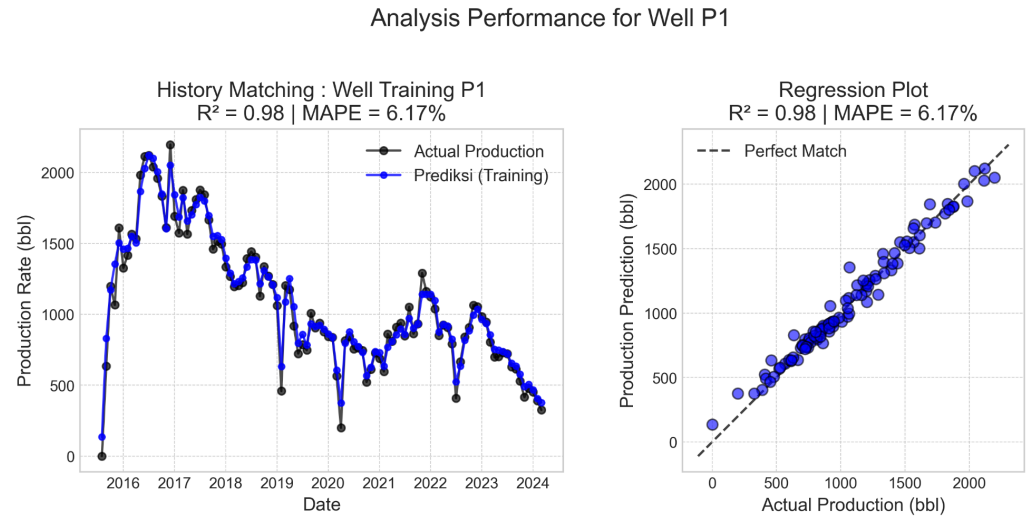

Figure 8 (a)

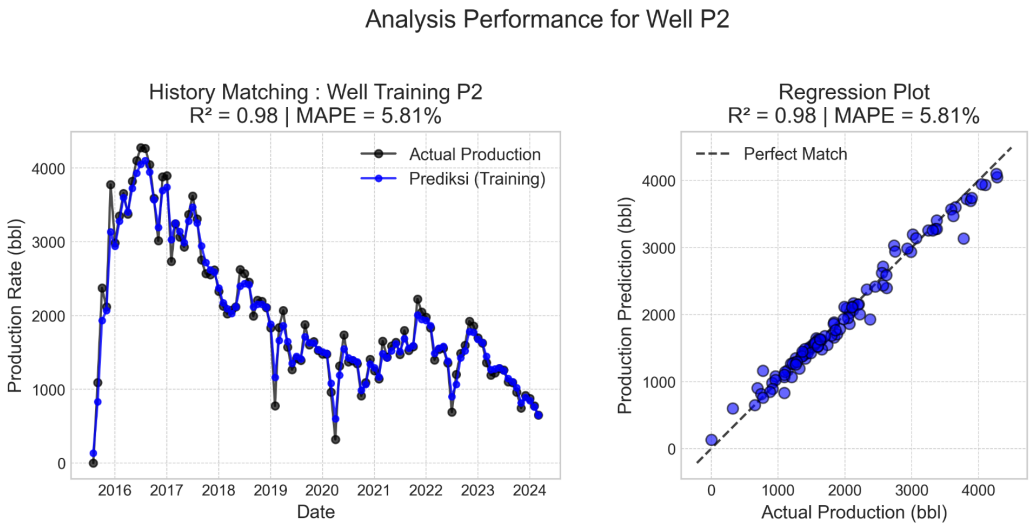

Figure 8 (b)

\

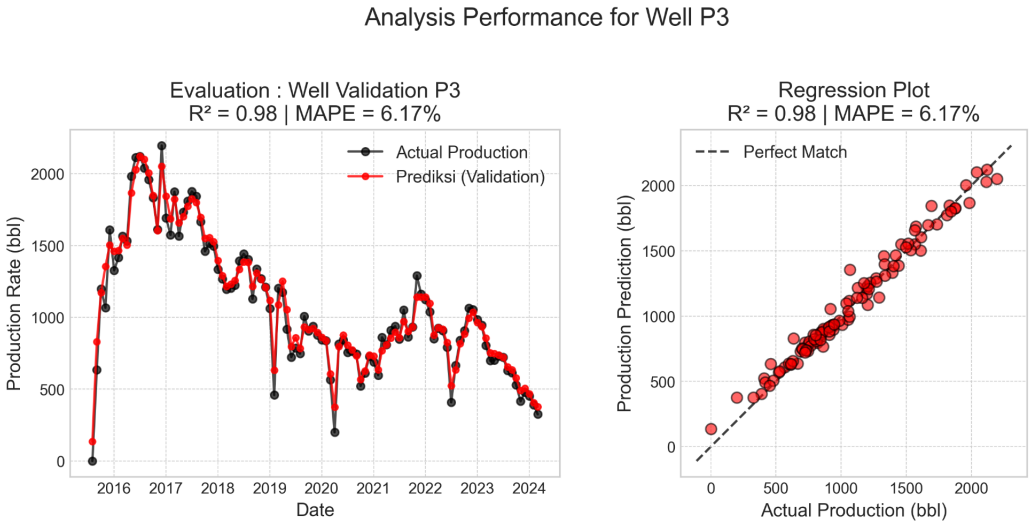

Figure 8 (c)

Figure 8. Random forest prediction performance for wells production (a) Well P1 (b) Well P2 (c) Well P3

of data points (which compares predicted values with actual values) is concentrated very tightly along the perfect prediction line (red dotted line). This visually confirms the near-perfect correlation and the absence of significant bias in the predictions. An XGBoost machine learning model was created as a benchmark for further validation, using an approach that has been proven effective in the oil and gas industry (Fajrul Haqqi et al., 2023; Simanjuntak & Irawan 2021). In Figure 9, this model is trained on P1 and P2 well data, then tested on P3 well data as validation data, in accordance with the data division methodology commonly used in machine learning applications for reservoir prediction (I. D. R. Nugroho et al., 2024).

The performance analysis results show that on the training data (P1 and P2), the model achieved a near-perfect fit with $R^2 = 1.00$ and MAPE < 1%, which is consistent with the XGBoost performance reported in similar studies (Hafidz & Fauzi, 2025). More importantly, on the previously unseen validation data (P3), the model maintained very high accuracy with $R^2 = 0.86$ and MAPE = 0.86%.

The outstanding performance on this validation set indicates that the model effectively captured the underlying production patterns without overfitting, consistent with findings from XGBoost-based research for reservoir property estimation (Fajrul Haqqi et al., 2023). These results provide strong evidence that production reinforces the effectiveness of the machine learning approach for production forecasting (Noshi et al., 2019), thereby validating the trends identified by previous models.

Hydrolyzed polyacrylamide (HPAM)

HPAM is the most used polymer in EOR applications. It gives significantly greater recovery of oil as it exhibits greater visco-elasticity than Xanthan solutions. The polyacrylamide adsorbs strongly on the mineral surface and makes the polymer partially hydrolyzed, and hence reduces adsorption by reacting the polyacrylamide with base. The EOR process is time-consuming, which increases the need for polymer stability. In general, hydrolysis should not exceed 40% in a period of three months, although acidic or basic conditions tend to speed up the process. HPAM also lacks tolerance when exposed to high temperatures or high salinity (Mbise 2019). The effectiveness of synthetic polymer flooding in improving sweep efficiency has been well documented in laboratory studies. It has been demonstrated that HPAM-based polymers can significantly enhance mobility control, although their performance is heavily influenced by reservoir temperature and salinity, which may reduce viscosity stability. This highlights the importance of rigorously validation of polymer performance under complex reservoir conditions, as addressed in this study using CRM and machine–learning–based diagnostic approaches. (Auni et al., 2023).

Forecast for polymer injection

Figure 10 presents the historical and forecasted water injection rates for wells I-F-4 and I-F-5. The historical period (up to 2024) shows fluctuations in the actual injection data. For the forecast period (starting in 2025), the injection rate for both wells is maintained at a constant level of 1,500 STB/day.

Figure 11 presents the oil production rate forecast for the 3,000 ppm polymer injection scenario across the three main production wells. After a period of fluctuating history matching (before 2025), the implementation of polymer injection resulted in a flatter and more sustainable production decline curve.This demonstrates the effectiveness of polymers in improving sweep efficiency and reducing the rate of decline. Well P-F-14 (blue) shows the most stable production profile, while P-F-11B (red) experiences the fastest decline. This combined profile represents the optimal EOR scenario that produces the highest Recovery Factor.

Figure 12 presents a comparison of water cut between the base case and the 3,000 ppm polymer injection scenarios. During the forecast period (after 2025), the polymer scenario clearly produces a lower water cut in all three wells. This shows that the polymer does improve the mobility ratio, delay water breakthrough, and boost sweep efficiency, thereby contributing to the observed increase in oil production rate (Palyanitsina et al., 2022).

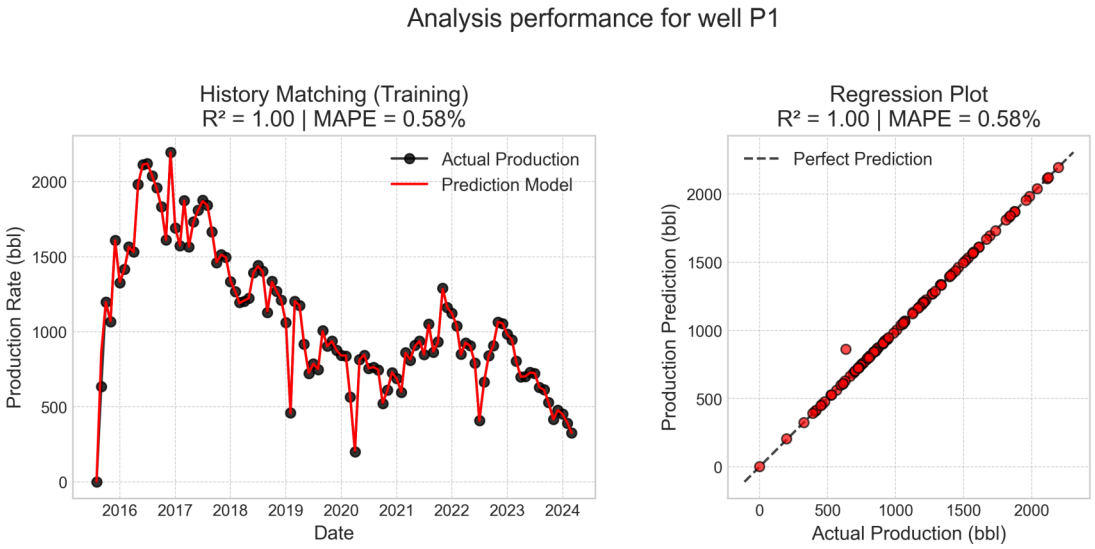

Figure 9 (a)

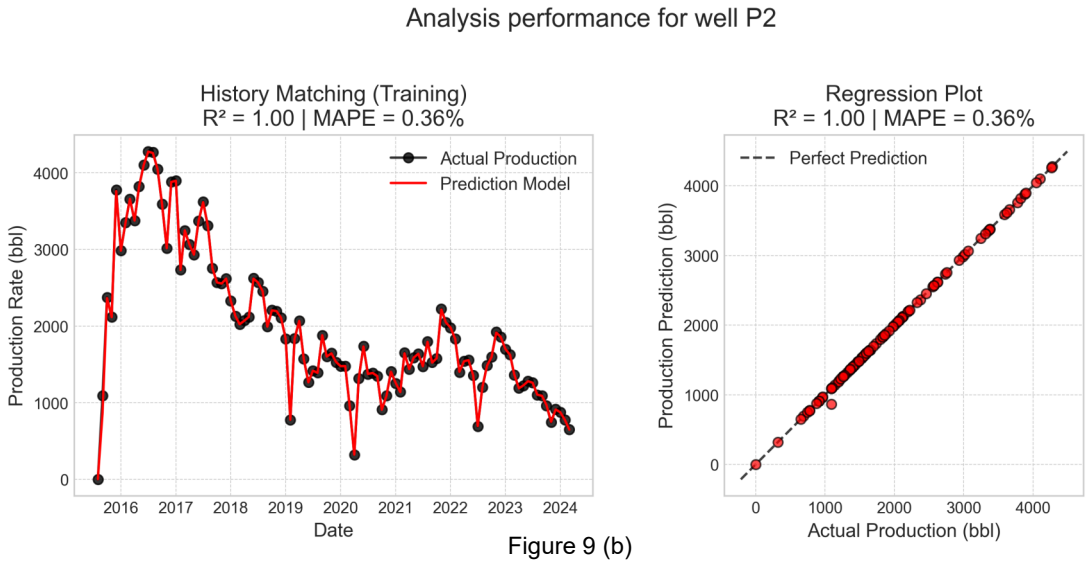

Figure 9 (b)

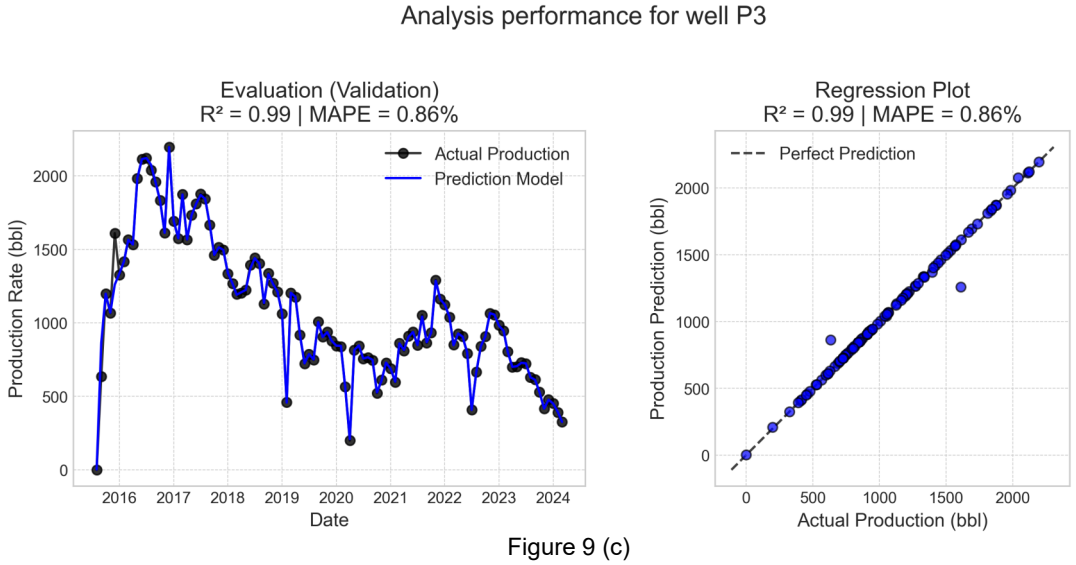

Figure 9 (c)

Figure 9. XGBoost prediction performance for wells production (a) Well P1 (b) Well P2 (c) Well P3

Figure 13 presents the cumulative oil production for both the base waterflood case and the polymer injection scenario. During the history matching period, both curves overlap, indicating identical reservoir performance prior to polymer injection. After the onset of polymer injection, the polymer scenario exhibits a higher cumulative oil production, resulting in an incremental oil gain of approximately 0.138 MMSTB. Although this increase confirms the effectiveness of polymer flooding, the relatively small magnitude highlights the limited improvement in sweep efficiency caused by reservoir heterogeneity and polymer retention effects.

Table 5. Polymer injection scenario

Scenario	Oil Cumulative	RF%
Scenario 0 ppm	16,25	21,12
Scenario 1000 ppm	16,32	21,20
Scenario 1500 ppm	16,34	21,23
Scenario 2000 ppm	16,36	21,26
Scenario 3000 ppm	16,39	21,30

The results of polymer injection simulations in the Volve field, as presented in Table 5, indicate that there is no significant improvement in the recovery factor (RF). The RF value only increased from 21.12% in the base scenario to 21.30% at a concentration of 3000 ppm, corresponding to a cumulative oil production increase from 16.25 MMSTB to 16.39 MMSTB.

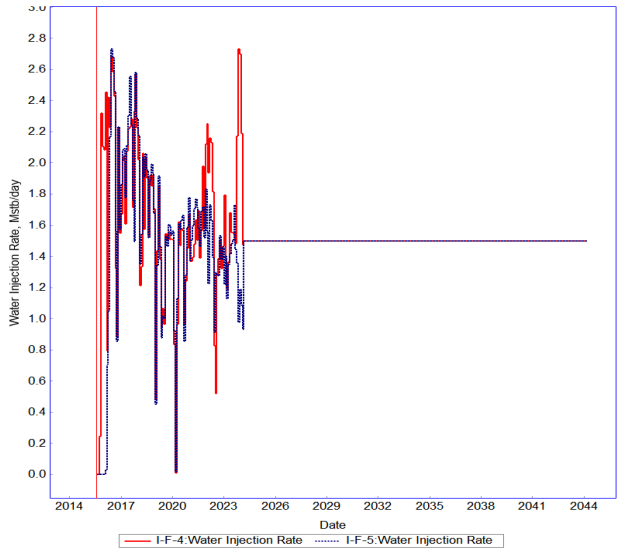

Figure 10. Historical and forecasted water injection rates for well injectors I-F-4 and I-F-5

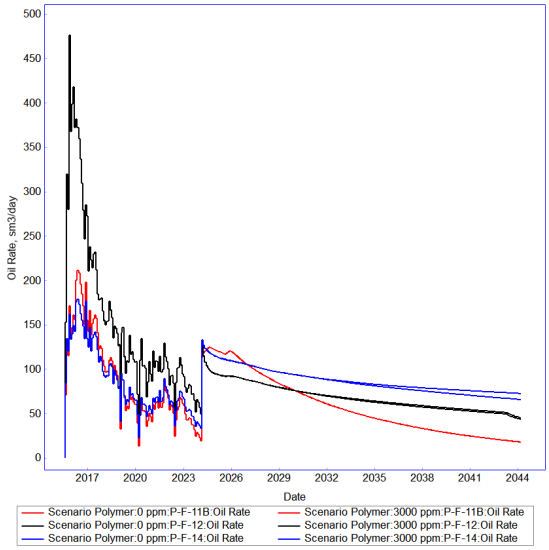

Figure 11. Forecasted oil production rates for production wells P-F-11B, P-F-12, and P-F-14 under the 3,000 ppm polymer injection scenario.

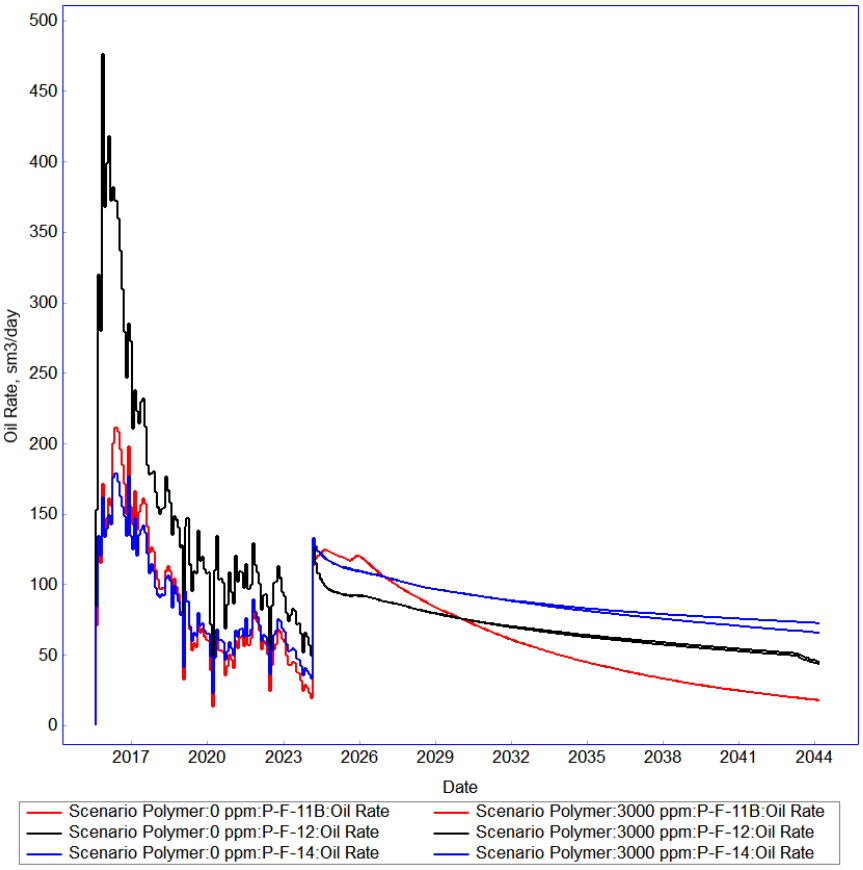

Figure 12. Comparison of water cut between the base waterflood case and the 3,000 ppm polymer injection scenario.

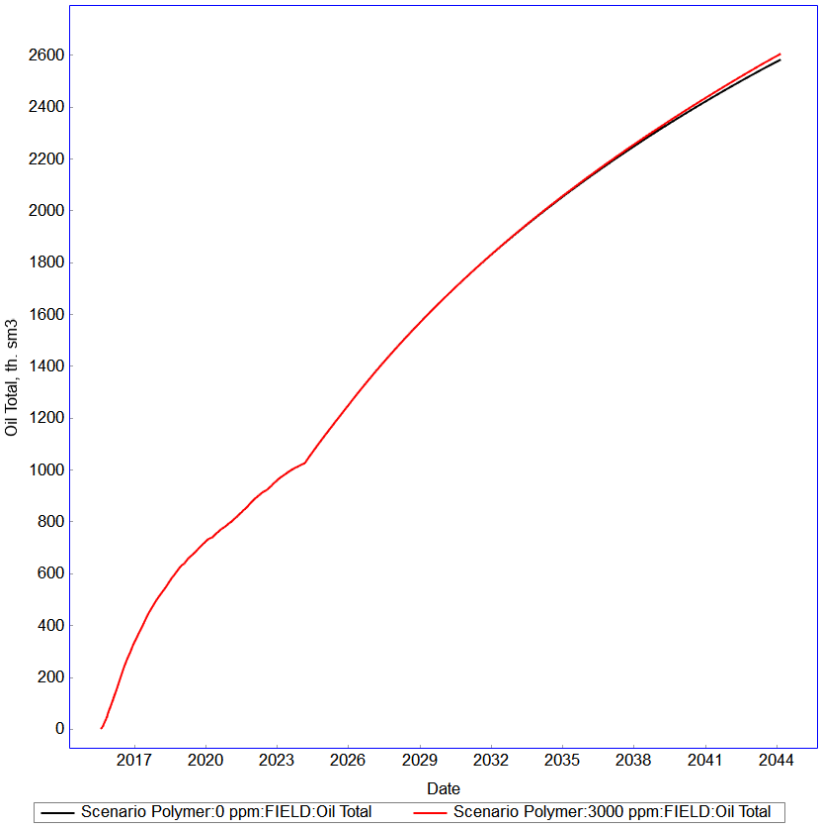

Figure 13. Cumulative oil production comparison between the base case and polymer injection scenario.

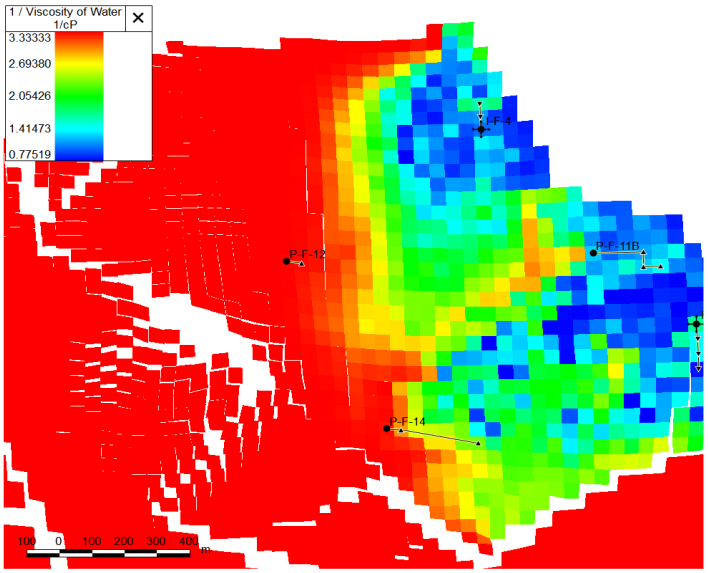

Figure 14. Water viscosity distribution after polymer injection.

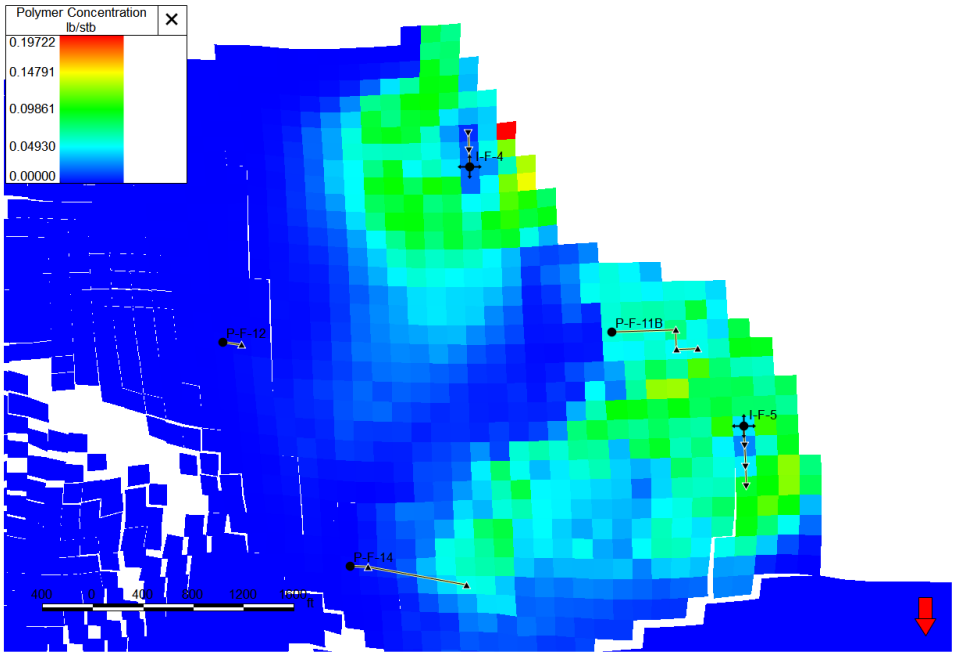

Figure 15. Polymer concentration distribution at the end of simulation Polymer Injection

This relatively small increase indicates that the performance of the polymer injection mechanism in the Volve field is limited due to reservoir characteristics that constrain the effectiveness of polymer fluids.

Figure 14 utilizes the 'Minimum' aggregation method to visualize the reservoir layer exhibiting the highest fluid viscosity. It is evident that the polymer successfully increased the viscosity to 1.29 cP (blue zone) compared to the baseline formation water viscosity of 0.3 cP (red zone). However, the polymer distribution is severely restricted, and it fails to reach the primary production wells. Given that this map represents the 'best-case' layer, it strongly suggests a channeling issue in which the polymer flows primarily through thin, high-permeability streaks while leaving the remaining oil in adjacent layers. This process explains why the total incremental oil recovery remains low, at 0.18%."

Figure 15 illustrates the distribution of polymer concentration at the end of the simulation. The visualization reveals that the polymer is primarily concentrated around the injection wells (I-F-4 and I-F -5) and the production well P-F-11B. Conversely, the remaining production wells (P-F-12 and P-F-14) and the majority of the inter-well area remain in the blue zone (0 lb/stb). The presence of polymer at producer

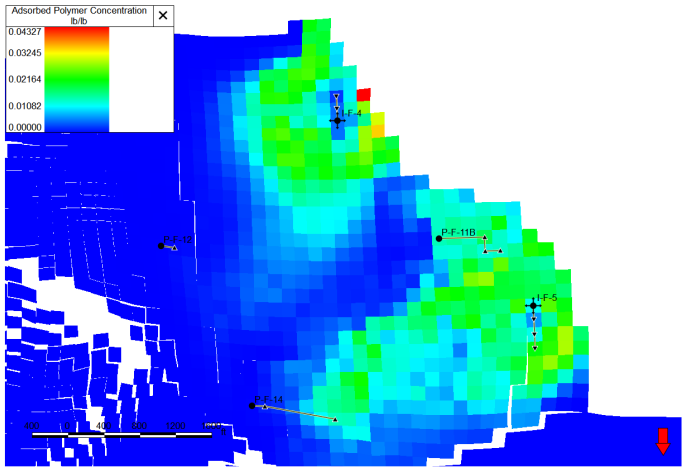

Figure 16. Distribution of adsorbed polymer concentration

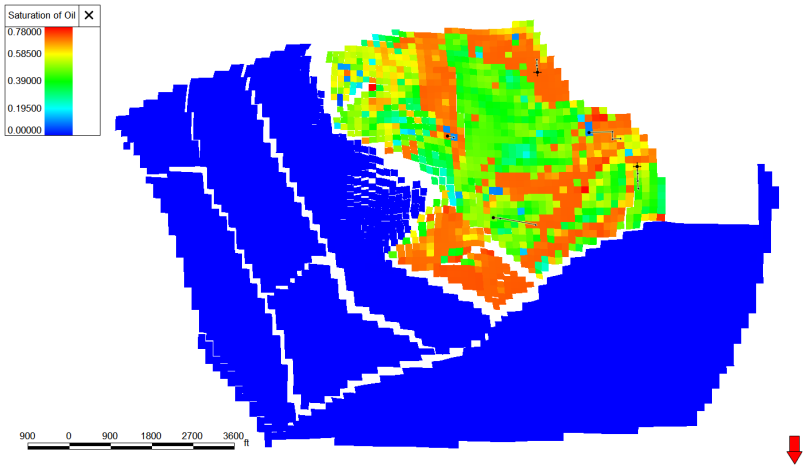

Figure 17. Oil saturation distribution after waterflooding

P-F-11B indicates a channeling issue or early polymer breakthrough, where the injected fluid followed a high-permeability path directly from the injector to this specific producer. Regarding the unswept areas, this observation indicates that a significant portion of the injected polymer was likely adsorbed by the formation rock, thereby impeding its transport to a wider area. Since the polymer was unable to sweep the inter-well zones effectively between the injectors and the remaining producers, significant oil displacement toward the production wells was not achieved. These combined factors-channeling and high retention-constitute the primary reasons for the minimal incremental recovery observed (0.18%)."

Figure 16 visualizes the distribution of adsorbed polymer concentration retained on the reservoir rock surface. The map exhibits high adsorption values (indicated by green and yellow zones) concentrated heavily in the immediate vicinity of the injection wells (I-F-4 and I-F-5). In contrast, the regions further into the reservoir and surrounding the production wells (P-F -12 and P-F-14) show negligible adsorption (blue zones), indicating that the polymer front never reached these areas. This visual evidence confirms that high polymer retention is a critical factor limiting the project's success. The injected polymer is rapidly consumed by the rock matrix due to adsorption near the wellbore, causing a severe 'chromatographic retardation' effect. This prevents the polymer bank from propagating deep into the inter-well zones to mobilize bypassed oil. Consequently, the effective viscosity within the reservoir remains low, directly explaining the marginal incremental oil recovery of 0.18%."

Figures 17 and 18 present the comparison of areal oil saturation maps at the end of the simulation period for the base case (waterflooding)

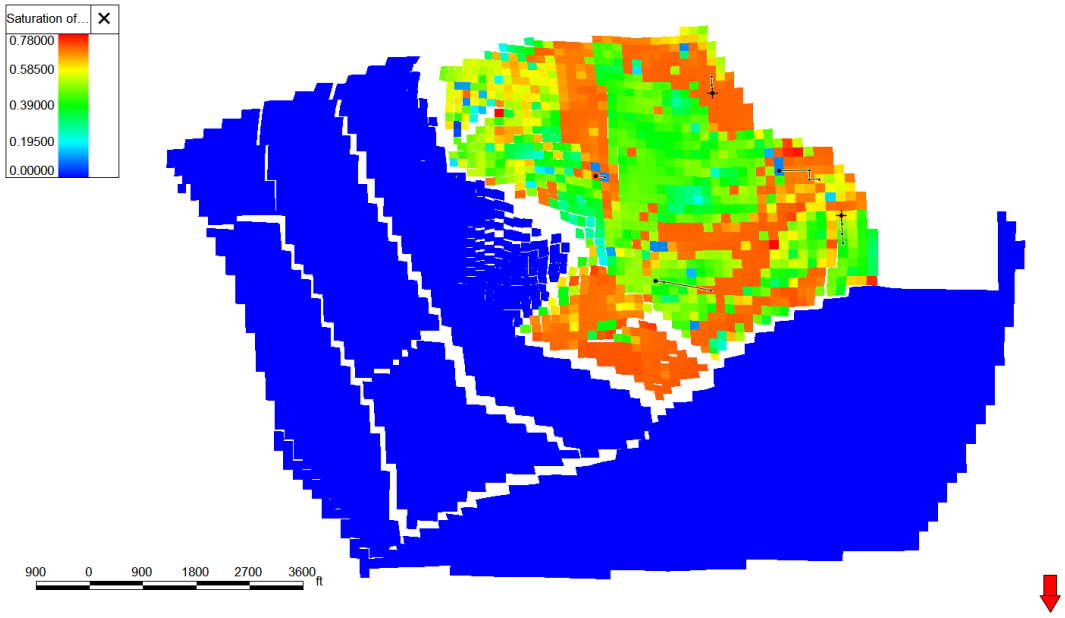

Figure 18. Oil saturation distribution after polymer flooding

and the polymer injection scenario, respectively. Visual observation reveals that the saturation profiles between the two scenarios are strikingly similar. Significant zones of by passed oil (indicated by red areas with $S_o > 0.60$) persist in the inter-well regions in both cases, indicating that the injected fluid followed similar preferential flow paths regardless of the injection type. This lack of visual contrast in the saturation maps suggests that the polymer injection did not significantly improve the macroscopic sweep efficiency. The expected mechanism of flow diversion—where the viscous polymer diverts flow from high-permeability swept zones into low-permeability unswept zones—did not occur effectively. This could be attributed to high polymer adsorption on the rock surface or insufficient viscosity contrast to overcome the reservoir heterogeneity. Consequently, this visual evidence strongly corroborates the production performance results, which showed a marginal incremental oil recovery of only 0.18%.

The inability of the polymer to expand the swept volume (as shown in Figure 18) physically explains the insignificant gain in cumulative oil production compared to the waterflood baseline. Based on the permeability distribution in Figure 3, the Volve field exhibits a relatively high degree of heterogeneity. Permeability values vary significantly, with red-orange areas indicating high-permeability zones (up to ±2000 mD), while yellow to green areas indicate zones with low permeability approaching zero. This condition leads to an imbalance in fluid flow during the injection process, where the polymer tends to flow through high-permeability streaks and bypass low-permeability regions without being effectively swept. As a result, sweep efficiency does not increase significantly, even though the viscosity of the injection fluid has been enhanced by the addition of polymer (Erfando et al., 2019). The high temperature of the reservoir, which is about 224.6°F (107°C), also breaks down the molecular chains of the hydrolyzed polyacrylamide (HPAM) polymer utilized in this simulation.

HPAM is known to have limited thermal stability, as at temperatures above 90–100°C the polymer chain structure begins to experience chain scission and excessive hydrolysis (Saputra et al., 2022), resulting in a decrease in molecular weight and a loss of ability to maintain solution viscosity. The polymer's efficacy in reducing the mobility ratio between water and oil is significantly reduced when viscosity decreases. The injected polymer fluid behaves almost like ordinary water in porous media and is unable to inhibit water fingering and channeling in high-permeability zones effectively. High salinity conditions and the presence of

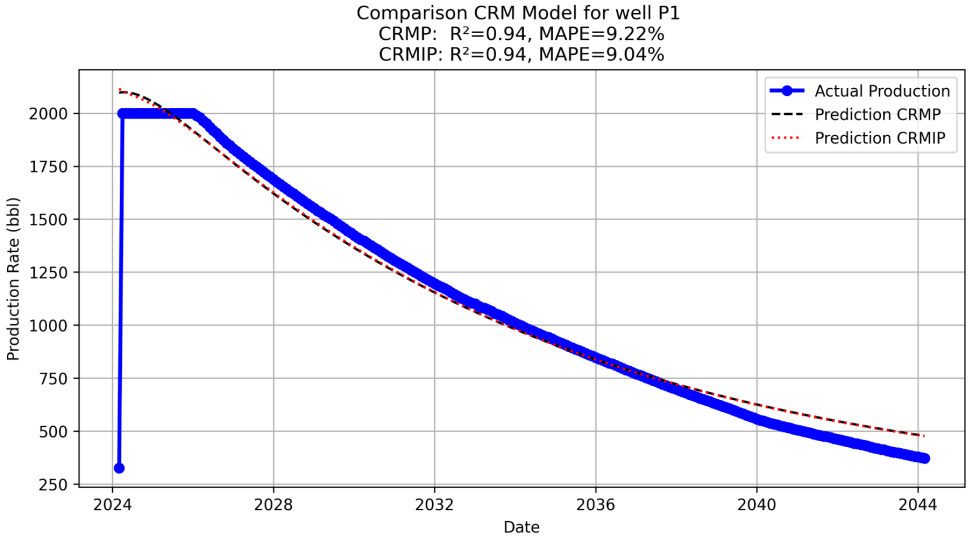

Figure 19(a)

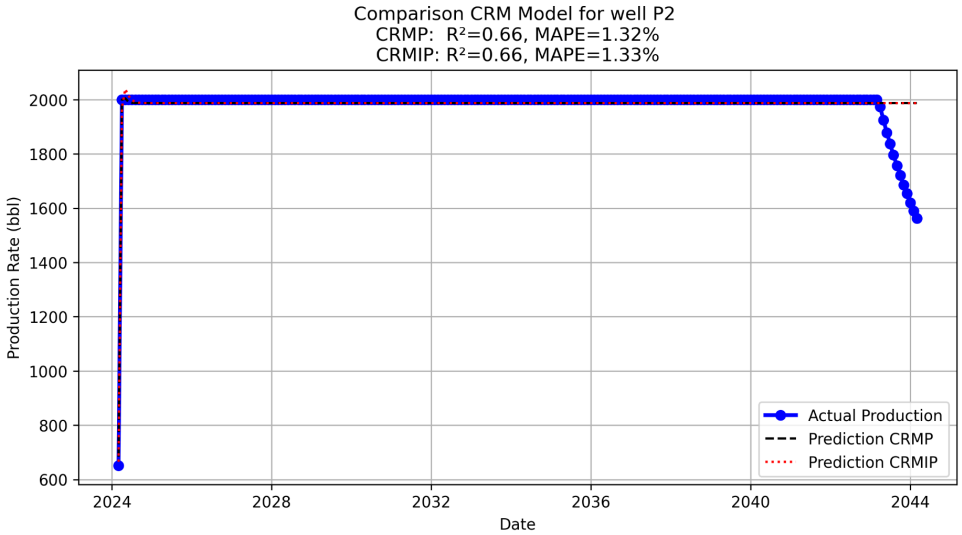

Figure 19(b)

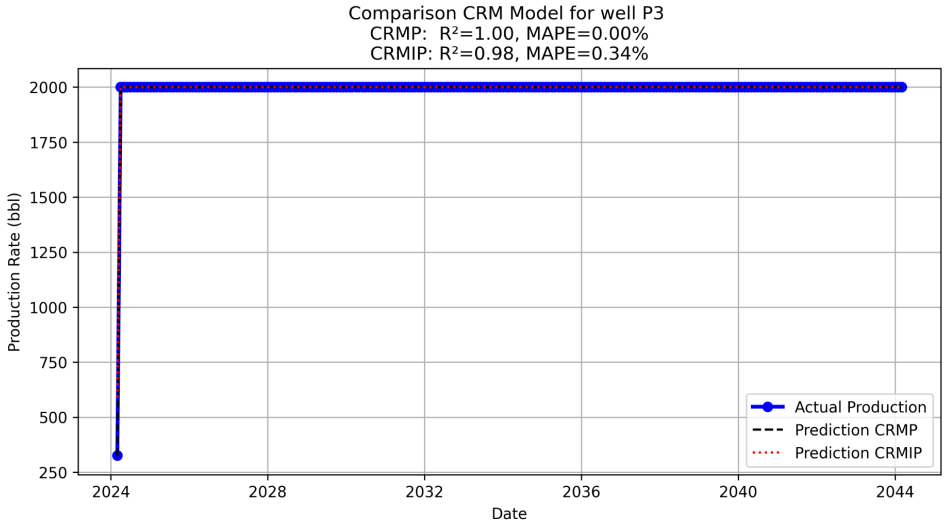

Figure 19(c)

Figure 19. CRM prediction after polymer injection in volve field (a) Well P1 (b) Well P2 (c) Well P3

divalent ions (Ca^{2+} and Mg^{2+}) in the Volve formation water further impair the polymer's performance. These ions interact with the polymer chains, leading to precipitation or coiling that diminishes the solution's hydrodynamic efficiency. In addition, polymer adsorption onto the surface of sand grains causes most of the polymer to remain around the injection zone, allowing only a limited amount to reach the production zone. Consequently, the improvement in sweep efficiency becomes localized and restricted to certain areas of the reservoir.

Analysis of the water cut trends in Figure 12 supports these findings. In the base scenario without polymer (0 ppm), the water cut increases rapidly after the initial production period and reaches more than 80% in 2035, indicating the dominance of water production in the production well. Conversely, in the 3000 ppm polymer injection scenario, the rate of increase in water cut is slower and tends to stabilize in the range of 70–75% in the same period. This shows that even though the increase in RF is not significant, polymers nonetheless have an important function in controlling the rate of injection water movement by increasing fluid viscosity and decreasing the mobility ratio (Pramadika et al., 2019).

Thus, polymer injection still contributes to delaying water breakthrough and mitigating the rate of water cut increase in some wells, especially in zones with high permeability. However, the water control effect is temporary and local, as reservoir heterogeneity causes uneven polymer distribution. In high-permeability pathways, the polymer is rapidly transported toward the production well, providing limited improvement in low-permeability zones. As a result, although the water cut improved slightly at the beginning of the injection period, the effect decreased over time, and water production increased again.

Overall, the simulation results show that polymer injection in the Volve Field has a positive effect on water control and production stability, but does not result in a significant increase in oil recovery. This phenomenon illustrates the diminishing return effect of polymer injection, where increasing polymer concentration is no longer proportional to the increase in recovery factor. The combination of high permeability heterogeneity, thermal degradation of polymers at 107°C, high formation salinity, and high adsorption is the main factor limiting the effectiveness of the mobility control mechanism in the Volve reservoir.

Analysis, history matching, and validation CRM for polymer injection

Figure 19 presents the final validation of the models CRMP and CRMIP by testing them against a predetermined polymer injection forecasting scenario. The objective is to ensure that these simplified analytical models can accurately replicate the results of complex enhanced oil recovery (EOR) scenarios at the individual well level (Sayarpour et al., 2009), as the effectiveness of the CRM approach in reservoir characterization and performance prediction has also been well documented in various previous studies (de Holanda et al., 2018). For wells P2 and P3, which represent injection-dominated plateau scenarios, themodel showed very high accuracy, with MAPE as low as 0.00% to 1.33%. Furthermore, the model also proved reliable in predicting the more complex decline scenario in Well P1, where the interaction between injection supportand natural decline occurs. In this case, the model remain produces strong predictions withresults of R^2 = 0.94 and MAPE = 9%.

Overall, the model's ability to accurately predict these vastly different production profiles provides high confidence that models can be used as an efficient proxy for EOR scenario optimization (Sayarpour et al., 2008). The regression plot analysis in Figure 20 provides strong visual validation for the polymer injection forecasting scenario. For Well P1, which represents the dynamic decline scenario, the data points are distributed linearly andclosely along the perfect prediction line, which is quantitatively confirmed by R^2 = 0.94 and MAPE = 9%. Conversely, for Wells P2 and P3, which represent the plateau (flat production) scenario, the regression plot shows the data clustered tightly at a single point (2000, 2000). This exceptional accuracy is evidenced by a very low MAPE (0.00% to 1.33%). It is important to note that the low R^2 value for P2 (0.66) is not an

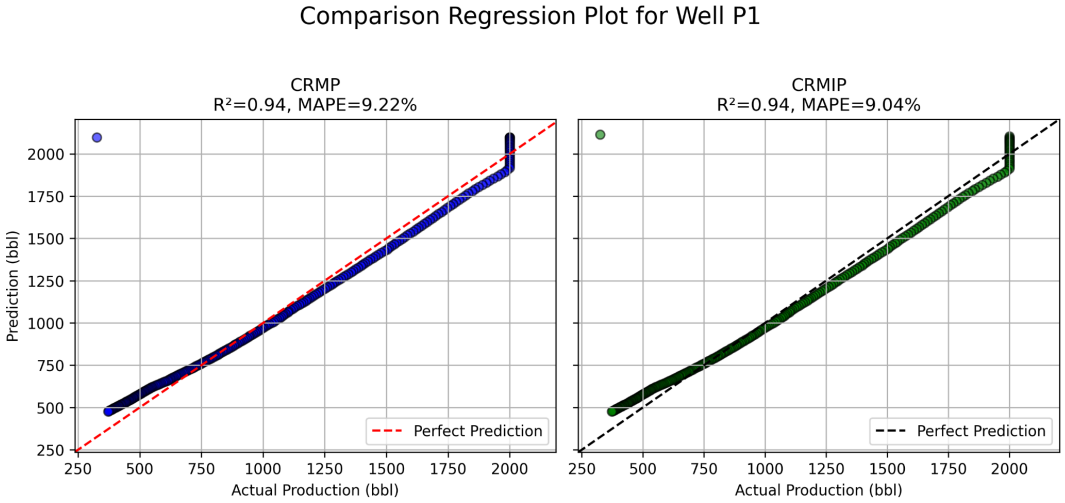

Figure 20 (a)

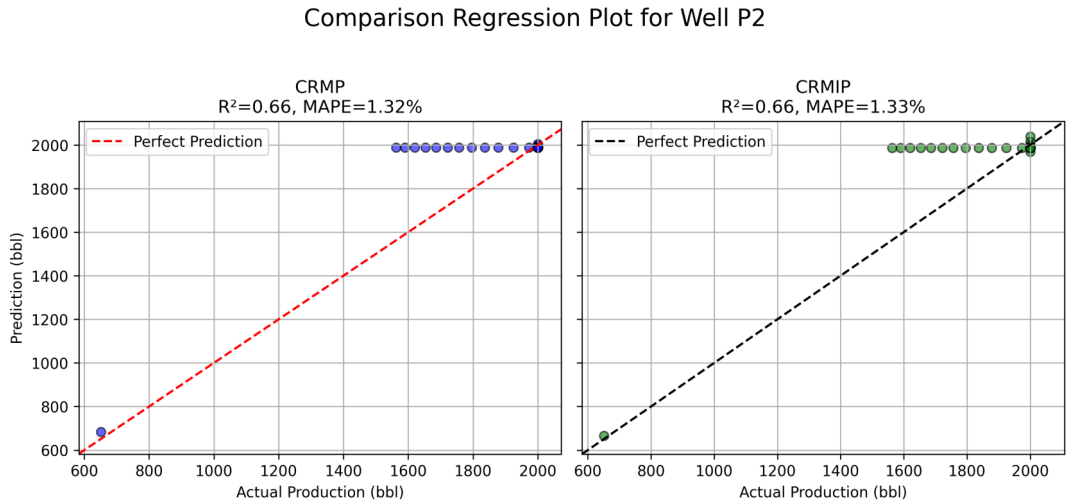

Figure 20 (b)

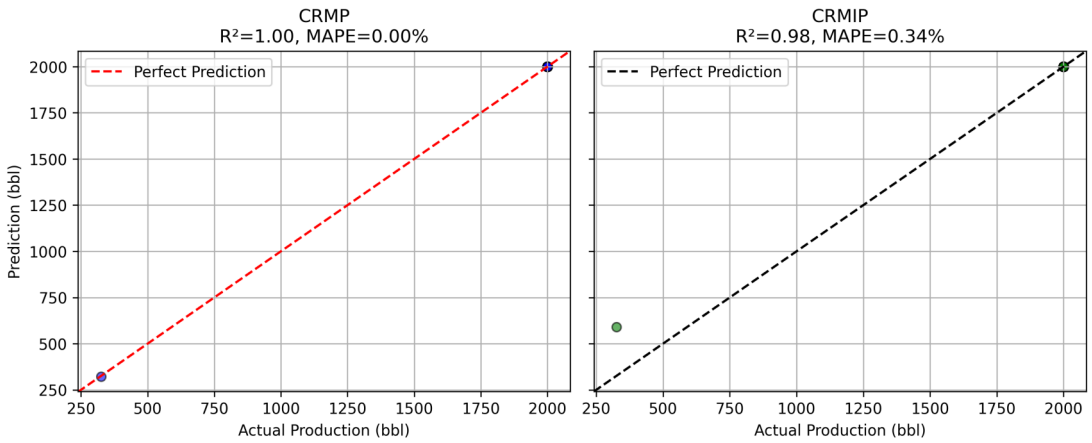

Figure 20 (c)

Figure 20. Comparison of regression plots for wells production after polymer injection
(a) Well P1 (b) Well P2 (c) Well P3

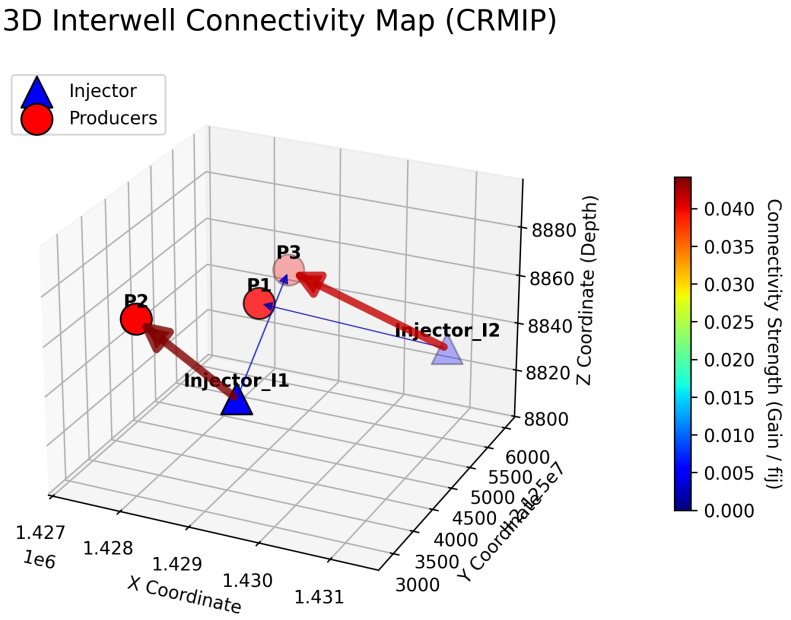

Figure 21. 3D interwell connectivity map derived from the CRMIP model after polymer injection.

indication of model failure, but rather a statistical deviation due to data validation with very low variance. Collectively, these plots visually confirm that both models have nearly identical performance and are highly reliable in replicating various forecasting profiles.

Table 6. Interwell connectivity and CRMP time constant after polymer injection

Well production	Well injection		Time constant τ (days)
	I1	I2	
P1	0.000015	0.000399	298.75
P2	0.023314	0.017766	32.25
P3	0.019998	0.023486	30.66

Table 7. Interwell connectivity of CRMIP after polymer injection

Well production	Well injection	
	I1	I2
P1	0.0000	0.0018
P2	0.0442	0.0000
P3	0.0028	0.0414

Table 8. CRMIP time constant after polymer injection

Well production	Well injection	
	I1	I2
P1	43.67	68.48
P2	30.00	83.95
P3	30.00	30.15

Tables 6, 7, and 8 summarize the post-polymer injection CRM parameters. This comparison highlights the significant advantages of the CRMIP model (Tables 7 and 8) in modeling EOR scenarios. The CRMIP model distinctly captures significant changes in reservoir flow patterns. The emergence of zero connectivity (P1-I1 and P2-I2) indicates the successful blocking of channeling pathways. Along with this, there is a flow diversion marked by a very high connectivity strengthening in the P2-I1 and P3-I2 paths. This phenomenon is consistent with research on the effects of heterogeneity on sweep efficiency (Borovina et al., 2022; Ramadhan et al., 2023). Conversely, the CRMP model (Table 6) fails to capture this dynamic behaviour, as evidenced by the physically unrealistic time constant estimate for P1 (298.75 days). Therefore, CRMIP provides a more accurate and reliable representation of post-polymer reservoir conditions.

This finding aligns with previous studies emphasizing thatselecting the appropriate simulation model is crucial for understanding flow behavior in heterogeneous reservoirs after polymer injection (Ramadhan et al., 2020). Figure 21 shows a 3D visualization of inter-well connectivity after polymer injection, where the thickness of the arrows indicates flow strength (f_{ij}). The dominant pattern is seen from Injector I1 to Producer P2 as the

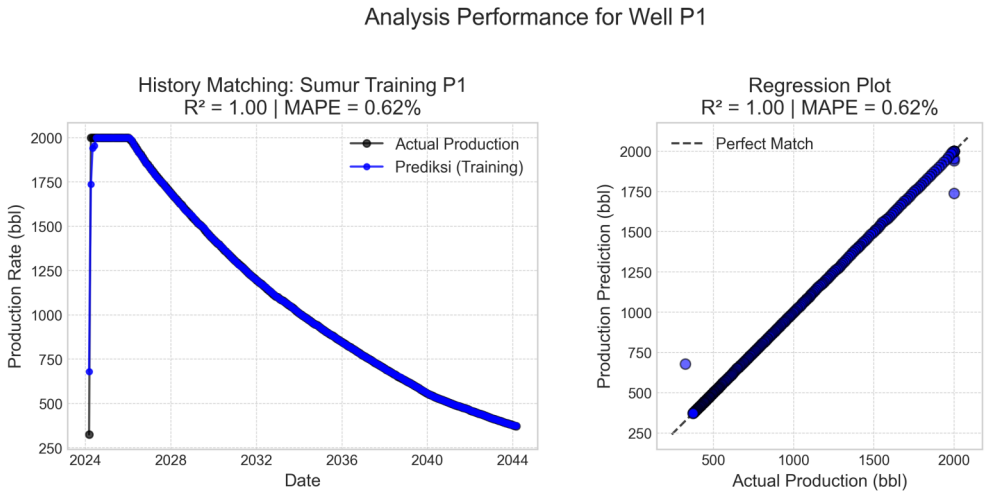

Figure 22. (a)

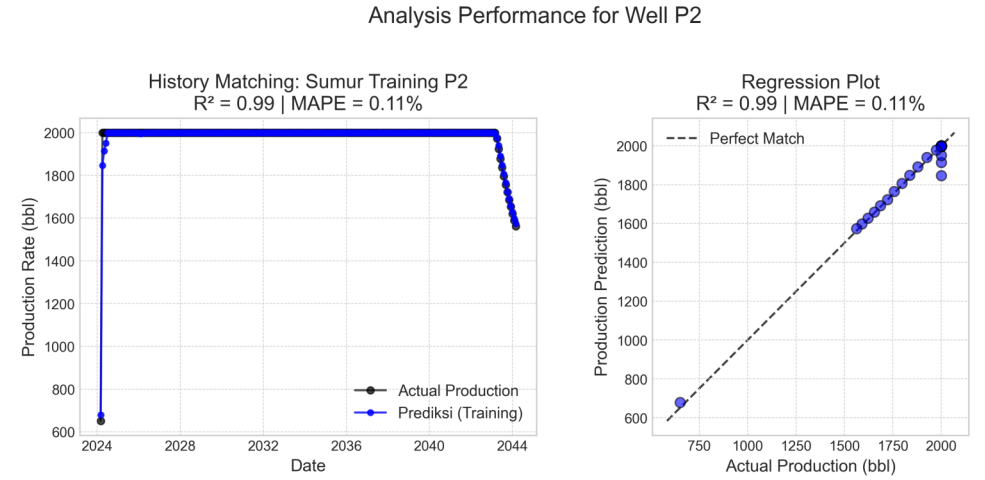

Figure 22. (b)

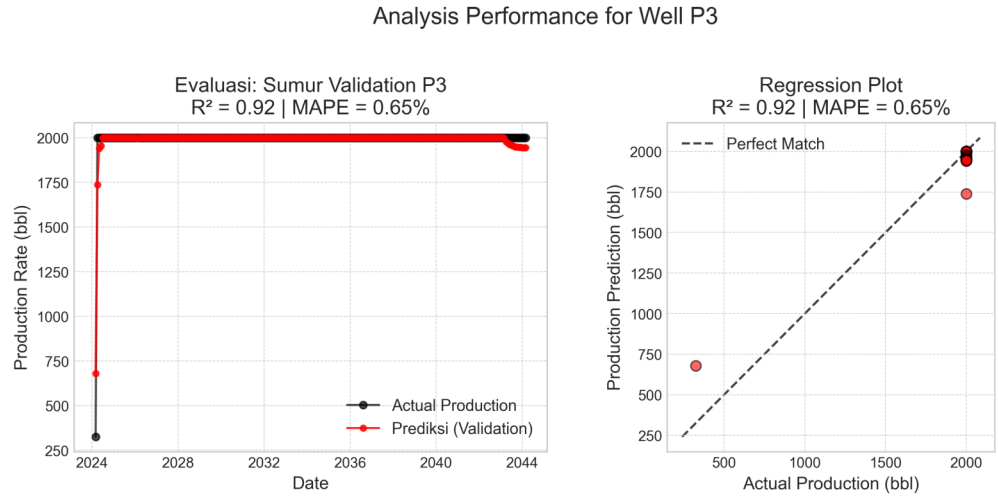

Figure 22. (c)

Figure 22. Random Forest performance analysis for wells production after polymer injection
(a) Well P1 (b) Well P2 (c) Well P3

strongest path, and from I2 to P1 and P3 as secondary flows. This pattern confirms the occurrence of effective flow diversion, with the polymer successfully increasing resistance in weak pathways and directing the fluid to the main production zones. Overall, this map demonstrates the success of the EOR intervention in modifying reservoir connectivity and increasing sweep efficiency.

Analysis machine learning random forest and gradient boosting for polymer injection

Figure 22 shows the results of the Random Forest model performance analysis on oil production rate predictions for three wells (P1, P2, and P3) after polymer injection. Each pair of graphs illustrates two main aspects, namely the history matching results between actual data and model predictions, as well as regression plots showing the level of conformity between actual data and predictions. The results show that the Random Forest model accurately represents production trends with a high degree of precision. R^2 value, which is close to 1, along with the low MAPE, demonstrates the model's ability to reliably predict changes in production due to the polymer injection process. This indicates that ensemble tree-based machine learning models, such as Random Forest, are very effective in capturing the nonlinear relationship between reservoir variables, injection parameters, and production response.

These findings are consistent with previous studies showing that combining the Random Forest algorithm with optimization techniques can improve the accuracy of oil and gas production predictions. In addition**, (**Rahmanifard & Gates 2024) also confirm that machine learning-based models, including Random Forest, can achieve high R^2 values in production forecasting for various reservoir types. Meanwhile, (Zhou et al., 2023) confirmed the effectiveness of Random Forest in predicting two-phase oil-water flow rates in horizontal wells, which is relevant to the context of predicting polymer injection performance in production wells.

Figure 23 shows the results of the XGBoost (Extreme Gradient Boosting) model performance analysis in predicting oil production rates after polymer injection for three wells: P1 and P2 as training data, and P3 as validation data. Each pair of graphs shows the results of history matching (left) and regression plots (right) between actual data and model predictions. The XGBoost model shows very high accuracy in reconstructing production trends. In well P1 with a decline pattern, the model achieved $R^2 = 0.99$ and MAPE < 3%, indicating its strong ability to capture production decline dynamics. Well, P2, which represents a plateau production pattern, also shows near-perfect prediction results ($R^2 = 0.97$, MAPE < 2%). For well P3 (validation data), the model remains stable with minimal deviation, demonstrating good generalization capabilities for unseen data and no evidence of overfitting.

The machine-learning models were validated using a well-based split, ensuring that the training and testing datasets originated from different wells to prevent overfitting. This process was further strengthened through 5-fold cross-validation, which ensured stable and consistent predictive performance. The very high R^2 value obtained by XGBoost (0.99) remains reasonable because the data used were derived from deterministic reservoir simulation results with minimal noise. The strong injection–production relationships in the dataset enable the model to learn reservoir dynamics with high accuracy. Residual analysis also showed no systematic bias, confirming that the model's strong performance was not caused by overfitting.

These results are consistent with recent studies demonstrating the effectiveness of the XGBoost algorithm in predicting oil and gas production performance based on field data.(A. Al Shabaan & N. Nemer, 2024compared XGBoost with Decision Tree and Random Forest and found that XGBoost achieved the highest prediction accuracy for oil and gas production data. Furthermore, (Hou et al., 2024) developed an adaptive fusion-based prediction method that integrates XGBoost to capture nonlinear relationships in unconventional well production data with highly accurate results. The research conducted by (Zhu et al., 2024) also reinforces these findings by showing that the XGBoost model is capable of predicting production trends with a very low error, even when applied to data with high noise levels. In general, these results confirm that XGBoost is a reliable and efficient

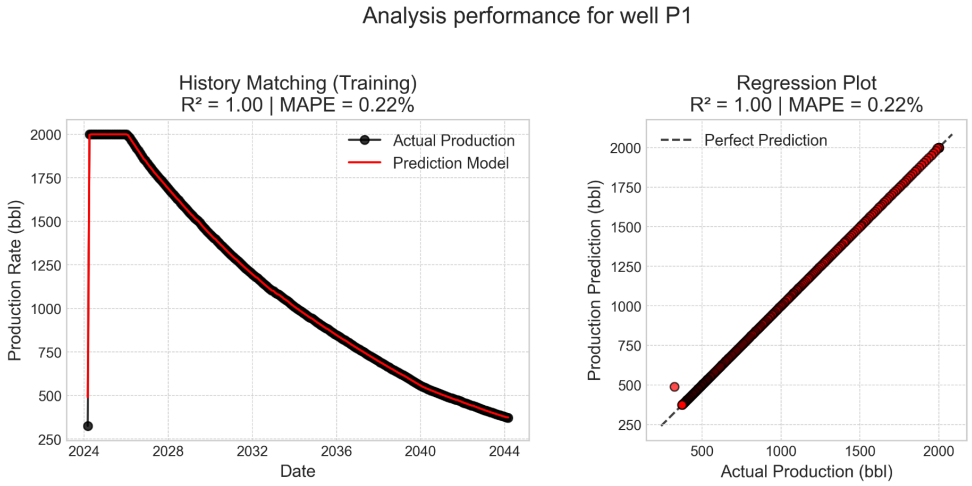

Figure 23. (a)

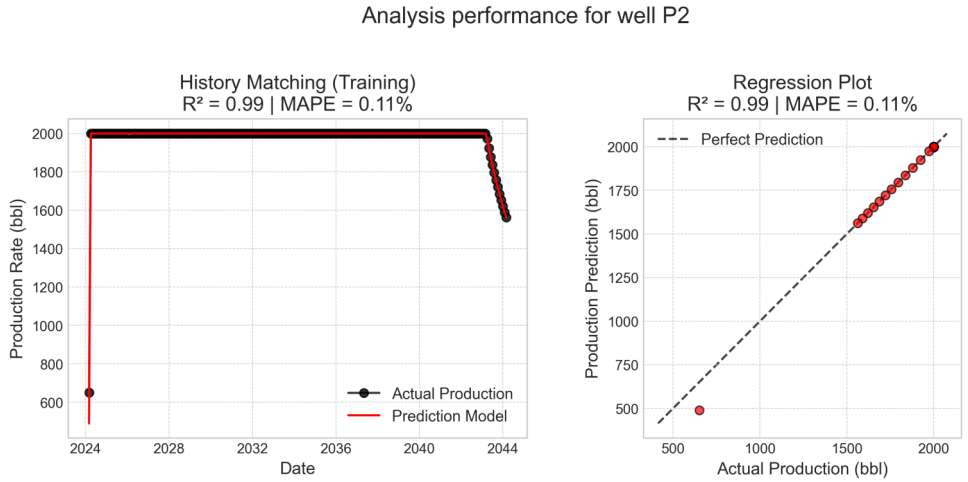

Figure 23. (b)

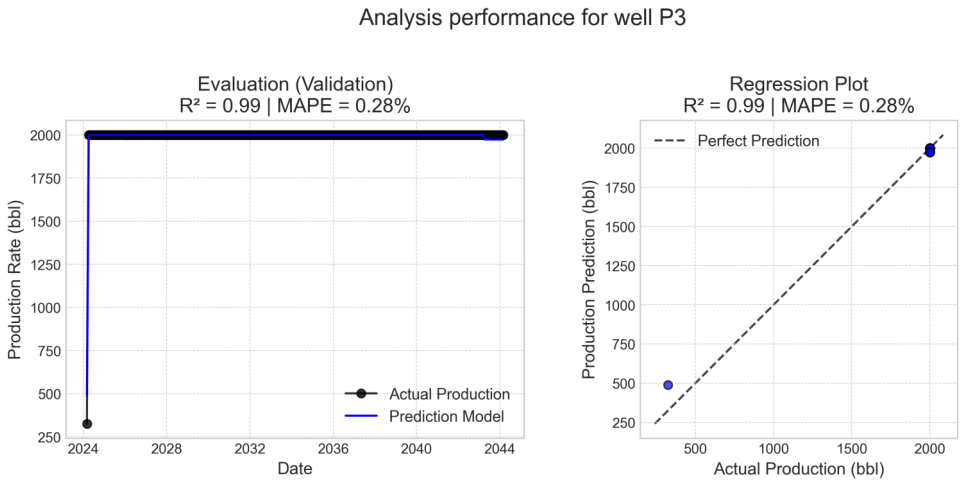

Figure 23. (c)

Figure 23. XGBoost performance analysis for wells production after polymer injection
(a) Well P1 (b) Well P2 (c) Well P3

machine learning approach for forecasting enhanced oil recovery (EOR) performance based on field data.

CONCLUSION

This study evaluated the performance of HPAM polymer injection in the Volve Field by validating tNavigator full-physics simulation results using the Injector–Producer configuration of the capacitance resistance model (CRM-IP) and machine-learning algorithms. The simulation results indicate that polymer injection increased the oil recovery factor from 21.12% to 21.30%, reflecting a measurable but modest improvement in sweep efficiency. CRM-IP successfully reconstructed production trends and quantified interwell connectivity (R^2 = 0.94; MAPE < 10%), providing clear insights into the influence of each injector on producer wells. Additional validation using machine-learning models demonstrated very high predictive accuracy (XGBoost R^2 = 0.99; MAPE < 1%), reinforcing the consistency and reliability of the simulation outcomes. The modest recovery improvement is primarily attributed to reservoir heterogeneity, HPAM degradation at 107°C, and formation salinity effects that reduce polymer viscosity stability. Overall, CRM-IP and machine learning serve as effective independent validation pathways that enhance confidence in polymer-injection evaluation and field planning.

ACKNOWLEDGMENT

The authors would like to thank the Laboratory of the Petroleum Engineering Study Program, Faculty of Engineering, Islamic University of Riau, and PT Pertamina Hulu Rokan.

GLOSSARY OF TERMS

Unit	Definition	Symbol
CRM	Capacitance Resistance Model	
DCA	Decline Curve Analysis	
f_{ij}	Coefficient Connectivity injection, producer	
τ	Time Constant	days
HPAM	Hydrolyzed Polyacrylamide	
RF	Recovery Factor	%
MAPE	Mean Absolute Percentage Error	%
I1, I2,etc	Injection Well 1, 2, etc	
MMSTB	Million Stock Tank Barrels	
PPM	Parts Per Million	
P1, P2, etc	Production Well 1,2, etc	
XGBOOST	eXtreme Gradient Boosting	
R^2	Coefficient Determination	
EOR	Enhanced Oil Recovery	

REFERENCES

A. Al Shabaan, M., & N. Nemer, Z. (2024). Oil and Gas Production Forecasting Using Decision Trees, Random Forest, and XGBoost. Journal of Al-Qadisiyah for Computer Science and Mathematics, 16(1), 9–20. https://doi.org/10.29304/jqcsm.2024.16.11431

Abbasov, A. A., Abbasov, E. M., & Suleymanov, A. A. (2023). Estimation of the waterflooding process efficiency based on a capacitive-resistive model with a nonlinear productivity index. 1(1), 19–26. https://doi.org/http://dx.doi.org/10.5510/OGP2023SI100820

Alvarado, V., & Manrique, E. (2010). Enhanced Oil Recovery: An Update Review. 1529–1575. https://doi.org/10.3390/en3091529

Auni, N. R., Afdhol, M. K., Ridha, M., & Erfando, T. (2023). Potensi Polimer Sintetik Sebagai Bahan Chemical Enhaced Oil Recovery Untuk Meningkatkan Sweep Efficiency pada Skala Pengujian Laboratorium. 57(1), 11–23.

Borovina, A., Hincapie, R. E., Clemens, T., Hoffmann, E., & Wegner, J. (2022). Selecting EOR Polymers through Combined Approaches—A Case for Flooding in a

Heterogeneous Reservoir. Polymers, 14(24). https://doi.org/10.3390/polym14245514

Chicco, D., Warrens, M. J., & Jurman, G. (2021). The coefficient of determination, R-squared, is more informative than SMAPE, MAE, MAPE, MSE, and RMSE in regression analysis evaluation. PeerJ Computer Science, 7, 1–24. https://doi.org/10.7717/PEERJ-CS.623

Davudov, D., Malkov, A., & Venkatraman, A. (2020). Integration of capacitance resistance model with reservoir simulation. Proceedings - SPE Symposium on Improved Oil Recovery, April 18–22. https://doi.org/10.2118/200332-MS.

de Holanda, R. W., Gildin, E., Jensen, J. L., Lake, L. W., & Shah Kabir, C. (2018). A state-of-the-art literature review on capacitance resistance models for reservoir characterization and performance forecasting. Energies, 11(12). https://doi.org/10.3390/en11123368

Erfando, T., Rita, N., & Ramadhan, R. (2019). The Key Parameter Effect Analysis Of Polymer Flooding On Oil Recovery Using Reservoir Simulation. Journal of Geoscience, Engineering, Environment, and Technology, 4(1), 49. https://doi.org/10.25299/jgeet.2019.4.1.2107

Fajrul Haqqi, M., Saroji, S., & Prakoso, S. (2023). An implementation of the XGBoost algorithm to estimate effective porosity on well log data. Journal of Physics: Conference Series, 2498(1). https://doi.org/10.1088/1742-6596/2498/1/012011

Fu, L., Zhao, L., Chen, S., Xu, A., Ni, J., & Li, X. (2022). A Prediction Method for Development Indexes of Waterflooding Reservoirs Based on Modified Capacitance–Resistance Models. Energies, 15(18). https://doi.org/10.3390/en15186768

Hafidz, M., & Fauzi, E. (2025). A Comparative Study of Arima, XGBoost, and Hybrid Arima–XGBoost Approaches for Forecasting IT Project Demand. 8. https://doi.org/https://doi.org/10.31539/intecoms.v8i3.15848

Hidayat, F., & Astsauri, T. M. S. (2021). Applied random forest for parameter sensitivity of low-salinity water injection (LSWI). https://doi.org/https://doi.org/10.1016/j.aej.2021.06.096

Hou, D., Han, G., Chen, S., Zhang, S., & Liang, X. (2024). A Study on a Novel Production Forecasting Method of Unconventional Oil and Gas Wells Based on Adaptive Fusion. Processes, 12(11). https://doi.org/10.3390/pr12112515

Imankulov, T., Kenzhebek, Y., Makhmut, E., & Akhmed-Zaki, D. (2022). Using machine learning algorithms to solve the polymer flooding problem. European Conference on the Mathematics of Geological Reservoirs 2022, ECMOR 2022, 40(6), 35–40. https://doi.org/10.3997/2214-4609.202244056

Khalbia, D. (2021). Coupled Capacitance Resistance Model and Aquifer Model for Waterflood Performance Prediction.

Lesan, A., Ehsan Eshraghi, S., Bahroudi, A., Reza Rasaei, M., & Rahami, H. (2018). State-of-the-Art Solution of Capacitance Resistance Model by Considering Dynamic Time Constants as a Realistic Assumption. Journal of Energy Resources Technology, Transactions of the ASME, 140(1). https://doi.org/10.1115/1.4037368

Maurenza, F., Yasutra, A., & Tungkup, I. L. (2023). Production Forecasting Using the ARPS Decline Curve Model with The Effect of Artificial Lift Installation. Scientific Contributions Oil and Gas, 46 (1), 17–26. https://doi.org/10.29017/SCOG.46.1.1310

Mbise, P. K. (2019). Enhanced Oil Recovery for Norne Field E-Segment using Alkaline Surfactant-Polymer Flooding. August.

Noshi, C. I., Eissa, M. R., Abdalla, R. M., & Schubert, J. J. (2019). An intelligent data-driven approach for production prediction. Proceedings of the Annual Offshore Technology Conference, 2019-May. https://doi.org/10.4043/29243-ms

Nugroho, I. D. R., Trisna, M. D., & Saroji, S. (2024). An Implementation of XGBoost and Random Forest Algorithm to Estimate Effective Porosity and Permeability on Well Log Data at Fajar Field, South Sumatra Basin, Indonesia. Indonesian Journal of Applied Physics, 14(2), 271. https://doi.org/10.13057/ijap.v14i2.82901

Nugroho, M. H., Aslam, B., & Marhaendrajana, T. (2021). Capacitance Resistance Model (CRM)

Application To Rapidly Evaluate and Optimize Production in the Peripheral Waterflood Field, Pandhawa Field Case Study. PETRO:Jurnal Ilmiah Teknik Perminyakan, 10(3), 149–162. https://doi.org/10.25105/petro.v10i3.9827

Nwogu, I. C., Ayo, A., Asemota, O., & Ajibade, O. (2019). Successful application of capacitance resistance modeling to understand reservoir dynamics in a brown field waterflood – A Niger delta swamp field case study. Society of Petroleum Engineers - SPE Nigeria Annual International Conference and Exhibition 2019, NAIC 2019. https://doi.org/10.2118/198819-MS

Palyanitsina, A., Safiullina, E., Byazrov, R., Podoprigora, D., & Alekseenko, A. (2022). Environmentally Safe Technology to Increase Efficiency of High-Viscosity Oil Production for the Objects with Advanced Water Cut. Energies, 15(3). https://doi.org/10.3390/en15030753

Pramadika, H., Samsol, S., & Satiyawira, B. (2019). The effect of the addition of polymer on the viscosity of the fluid for industrial oil and gas injection in the EOR method. Journal of Physics: Conference Series, 1402(2). https://doi.org/10.1088/1742-6596/1402/2/022053

Pyatibratov, P. V., & Zammam, M. (2023). Waterflooding optimization based on the CRM and solving the linear programming problem. 2(2), 59–67. https://doi.org/http://dx.doi.org/10.5510/10.5510/OGP2023SI200890

Rahmanifard, H., & Gates, I. (2024). A Comprehensive review of data-driven approaches for forecasting production from unconventional reservoirs: best practices and future directions. Artificial Intelligence Review, 57(8). https://doi.org/10.1007/s10462-024-10865-5

Ramadhan, R., Abdurahman, M., & Srisuriyachai, F. (2020). Sensitivity Analysis Comparison of Synthetic Polymer and Biopolymer using Reservoir Simulation. Scientific Contributions Oil and Gas, 43(3), 143–152. https://doi.org/10.29017/scog.43.3.516

Ramadhan, R., Novriansyah, A., Erfando, T., Tangparitkul, S., Daniati, A., Permadi, A. K., & Abdurrahman, M. (2023). Heterogeneity Effect on Polymer Injection: a Study of Sumatra Light Oil. Scientific Contributions Oil and Gas, 46(1), 39–52. https://doi.org/10.29017/SCOG.46.1.1322

Salehian, M., & Çýnar, M. (2019). Reservoir characterization using dynamic capacitance–resistance model with application to shut-in and horizontal wells. Journal of Petroleum Exploration and Production Technology, 9(4), 2811–2830. https://doi.org/10.1007/s13202-019-0655-4

Saputra, D. D. S. M., Prasetiyo, B. D., Eni, H., Taufantri, Y., Damara, G., & Rendragraha, Y. D. (2022). Investigation of Polymer Flood Performance in Light Oil Reservoir: Laboratory Case Study. Scientific Contributions Oil and Gas, 45(2), 81–86. https://doi.org/10.29017/SCOG.45.2.965

Sayarpour, M., Kabir, C. S., & Lake, L. W. (2008). Field applications of capacitance-resistive models in waterfloods. SPE Reservoir Evaluation and Engineering, 12(6), 853–864. https://doi.org/10.2118/114983-pa

Sayarpour, M., Zuluaga, E., Kabir, C. S., & Lake, L. W. (2009). The use of capacitance-resistance models for rapid estimation of waterflood performance and optimization. Journal of Petroleum Science and Engineering, 69(3–4), 227–238. https://doi.org/10.1016/j.petrol.2009.09.006

Shang, C., Ng, W., Nait, M., Jahanbani, A., & Struen, L. (2023). A Survey on the Application of Machine Learning and Metaheuristic Algorithms for Intelligent Proxy Modeling in Reservoir Simulation. Computers and Chemical Engineering, 170(December 2022), 108107. https://doi.org/10.1016/j.compchemeng.2022.108107

Simanjuntak, R., & Irawan, D. (2021). Applying Artificial Neural Network and XGBoost to Improve Data Analytics in the Oil and Gas Industry. Indonesian Journal of Energy, 4(1), 26–35. https://doi.org/10.33116/ije.v4i1.103

Weber, D. (2009). The Use of Capacitance-Resistance Models to Optimize Injection Allocation and Well Location in Water Floods. 292.

Yan, S., Li, W., Zhang, M., & Wang, Z. (2023). An Innovative Method for Hydraulic Fracturing Parameters Optimization to Enhance Production in Tight Oil Reservoirs. 1–24. https://doi.org/10.14800/IOGR.1262.

Zhao, W., & Liu, T. (2023). Approaches of Combining Machine Learning with NMR-based Pore Structure Characterization for Reservoir Evaluation. https://doi.org/10.20944/preprints202312.0444.v1.

Zhou, H., Liu, J., Fei, J., & Shi, S. (2023). A Model Based on the Random Forest Algorithm That Predicts the Total Oil–Water Two-Phase Flow Rate in Horizontal Shale Oil Wells. Processes, 11(8). https://doi.org/10.3390/pr11082346.

Zhu, R., Li, N., Duan, Y., Li, G., Liu, G., Qu, F., Long, C., Wang, X., Liao, Q., & Li, G. (2024). Well-Production Forecasting Using Machine Learning with Feature Selection and Automatic Hyperparameter Optimization. Energies, 18(1). https://doi.org/10.3390/en18010099.